

The Dwarf Spheroidal Companions to M31: WFPC2 Observations of Andromeda I¹

G. S. Da Costa

Mount Stromlo and Siding Spring Observatories, The Australian National University, Private Bag, Weston Post Office, ACT 2611, Australia

T. E. Armandroff

*Kitt Peak National Observatory, National Optical Astronomy Observatories²,
P.O. Box 26732, Tucson, Arizona 85726*

Nelson Caldwell

F. L. Whipple Observatory, Smithsonian Institution, P.O. Box 97, Amado, Arizona 85645
and

Patrick Seitzer

Department of Astronomy, University of Michigan, Ann Arbor, Michigan 48109

Accepted for Publication in the Astronomical Journal, December 1996 issue

¹Based on observations with the NASA/ESA *Hubble Space Telescope*, obtained at the Space Telescope Science Institute, which is operated by the Association of Universities for Research in Astronomy, Inc., (AURA), under NASA Contract NAS 5-26555.

²The National Optical Astronomy Observatories are operated by AURA, Inc., under cooperative agreement with the National Science Foundation.

ABSTRACT

Images have been obtained with the *Hubble Space Telescope* WFPC2 camera of Andromeda I, a dwarf spheroidal (dSph) galaxy that lies in the outer halo of M31. The resulting color-magnitude diagrams reveal for the first time the morphology of the horizontal branch in this system. We find that, in a similar fashion to many of the galactic dSph companions, the horizontal branch (HB) of And I is predominantly red. Combined with the metal abundance of this dSph, this red HB morphology indicates that And I can be classified as a “second parameter” system in the outer halo of M31. This result then supports the hypothesis that the outer halo of M31 formed in the same extended chaotic manner as is postulated for the outer halo of the Galaxy.

In addition to the red HB stars, blue HB and RR Lyrae variable stars are also found in the And I color-magnitude diagram. The presence of these stars indicates that And I contains a minority population whose age is comparable to that of the galactic globular clusters. We estimate, however, that the bulk of the stellar population in And I is ~ 10 Gyr old. Thus, again like many of the galactic dSphs, there is clear evidence for an extended epoch of star formation in And I. A radial gradient in the And I HB morphology has also been discovered in the sense that there are relatively more blue HB stars beyond the galaxy’s core radius. This may be evidence for more centrally concentrated star formation after the initial episode. Similar HB morphology gradients have also been identified in two of three galactic dSphs studied.

The mean magnitude of the blue HB stars suggests that And I lies along the line-of-sight at the same distance as M31 to within $\sim \pm 70$ kpc. Consequently, the true distance of And I from the center of M31 is between ~ 45 and ~ 85 kpc, with the higher estimates being more likely. Such distances are comparable to the galactocentric distances of the nearer Milky Way dSph companions Ursa Minor, Draco and Sculptor. From the mean color of the lower giant branch, the mean metal abundance of And I is estimated as $[\text{Fe}/\text{H}] = -1.45 \pm 0.2$ dex, while the presence of an internal abundance spread with total range of ~ 0.6 dex is suggested by the intrinsic color width of the upper giant branch. A small population of faint blue stars, which we identify as blue stragglers, is also present.

1. Introduction

The nine dwarf spheroidal (dSph) galaxy companions to our Galaxy are, because of their proximity, the most easily studied examples of what may be the most common type of galaxy in the Universe. These systems have been probed in greater and greater detail in the last decade, and though their evolutionary history is far from being completely understood, they are all now relatively well observed objects (see recent reviews, e.g. Da Costa 1992, Zinn 1993a, Mateo 1996). But within the Local Group there are at least three other objects that are classified as dwarf spheroidal galaxies: the dSph companions to M31. These galaxies, known as And I, II and III, lie at projected distances of ~ 45 , 130 and 60 kpc, respectively, from the center of M31. *Thus in the same way as the galactic dSphs are systems in the outer halo of the Galaxy, the And dSphs are systems in the outer halo of M31.*

Recent work on the And dSphs has established that there is a considerable degree of similarity between the M31 dSph system and that of the Galaxy. For example, Caldwell *et al.* (1992) determined accurate surface brightness profiles for the And systems and used these data to show that they follow the same relations between absolute magnitude, central surface brightness and core radius as do the galactic dSphs (see also Armandroff 1994). Ground-based color-magnitude diagrams that cover the upper 2 or 3 magnitudes of the giant branch are also available for the three And systems: And I (Mould & Kristian 1990, hereafter MK90), And II (König *et al.* 1993, see also Armandroff 1994) and And III (Armandroff *et al.* 1993). These studies permit estimates of the mean abundance³, the distance, and the intermediate-age population fraction for these galaxies. All three systems appear to be at, or close to, the distance of M31 and the mean abundances range from $[\text{Fe}/\text{H}] \approx -2.0$ for And III to $[\text{Fe}/\text{H}] \approx -1.4$ for And I. Further, the three dSphs follow the same relation between mean abundance and absolute magnitude as do the galactic dwarf spheroidals. As for intermediate-age population fraction, Armandroff *et al.* (1993) find $10 \pm 10\%$ for And I and And III, but for And II this fraction is not yet well established. However, since intermediate-age upper-AGB carbon stars have been identified in

this system (Aaronson *et al.* 1985, see also Armandroff 1994), the intermediate-age population fraction for this dSph is undoubtedly larger than that for And I or And III.

Apart from age determinations via measurement of turnoff luminosities, the major characteristic of the M31 dSphs that is lacking compared to the galactic dSphs, is information on the morphology of their horizontal branches. The galactic dSphs exhibit a wide range of horizontal branch (HB) morphologies. For example, the Draco and Ursa Minor systems have similar abundances and absolute magnitudes yet their HB morphologies are markedly different: that of Draco being much redder than that of Ursa Minor. Compared to the majority of galactic globular clusters of similar abundance to these systems, it is Draco that is anomalous. Draco is said to exhibit the so-called “second parameter effect” in possessing a redder HB than would be expected for its metal abundance. This second parameter effect is common among the Galaxy’s dSph companions and it is also particularly prevalent among the globular clusters that lie, like the dSphs, in the outer regions of the galactic halo.

Considerable effort has gone into attempting to understand the origin of the second parameter effect and its dependence on galactocentric distance. It is now generally accepted that the phenomenon is a manifestation of age differences that occur in the galactic halo (e.g. Lee, Demarque & Zinn 1994). Indeed this age difference interpretation of the diversity of HB types seen in the outer halo of the Galaxy is a cornerstone of the chaotic halo formation model advocated initially by Searle & Zinn (1978), in which the galactic halo is built out of the destruction of satellite galaxies over an extended interval of perhaps ~ 3 to 5 Gyr. *Does this prolonged formation scenario apply also to the halo of M31?* An initial attack on this problem can be made by determining the HB morphologies of the most readily identifiable objects in the outer halo of M31, the And dSph galaxies. Since the mean metal abundances of these systems are well established, we can accurately predict the HB morphology expected if the bulk of the stellar population in these galaxies is as old as the inner galactic halo globular clusters. If the observations reveal instead a diversity of HB morphologies, then it will be an indication that the outer halo of M31 may also have formed in the same drawn out chaotic manner as the outer regions of the halo of our galaxy.

³Unless otherwise qualified, the terms “abundance” and “[Fe/H]” should be understood as indicating the overall abundance of the elements heavier than hydrogen and helium.

We begin this task by presenting in this paper the results of a *Hubble Space Telescope* imaging study whose principal aim was to determine the HB morphology of the Andromeda I dwarf spheroidal galaxy. The observations, made with the WFPC2 camera, are detailed in the next section together with a description of the photometric analysis applied to the images. The resulting And I color-magnitude diagrams are discussed in detail in Section 3. The results, both in the context of the formation and the evolution of this dSph, and in the context of formation scenarios for the halo of M31, are discussed in Section 4 and summarized in Section 5.

2. Observations and Photometry

Andromeda I was imaged with the *Hubble Space Telescope* Wide Field Planetary Camera 2 (WFPC2, see Holtzman *et al.* 1995a for a complete description) on 1994 August 11 and again, at the same spacecraft orientation, on 1994 August 16. The first set of observations consisted of three 1800 sec integrations through the F555W (“Wide-V”) filter and six 1800 sec integrations through the F450W (“Wide-B”) filter, while the second set comprised four 1800 sec F555W and six 1800 sec F450W integrations. For the second set of observations (as executed) the HST pointing was set to place the center of And I, determined from the surface brightness study of Caldwell *et al.* (1992), on the center of the PC1 chip (*i.e.* aperture PC1-FIX). The first set of observations (as executed) however, was offset from this pointing by a small amount, nominally 20.5 PC pixels in both x and y , to facilitate investigation of the effects of image undersampling and small scale flat-fielding variations on the resulting photometry.

The observations were carried out successfully and the raw data frames were bias and dark subtracted, flat-fielded, etc, via the standard STScI “pipeline” process. The STSDAS task *gcombine* was then used to combine, removing cosmic rays, the individual frames into single “master” frames for each of the four filter and pointing combinations. Two details need to be discussed concerning this combination process. First, any pixels labeled as “bad” in the accompanying data quality files were flagged as such in the combined frames by setting their intensities to a constant value well below that of the “sky”. While this produces frames with obvious cosmetic defects, it is a better representation of the true data status than gener-

ating approximate intensities for bad pixels from their surrounds. Second, during the second set of F555W observations, the spacecraft drifted systematically by a small amount such that the positions of stars on the last frame differ from those on the first frame by ~ 0.5 PC pixels in both x and y . Such systematic drifts did not occur during any of the other sets of observations; in these cases the positions of the brighter stars on the individual frames are constant to better than 0.1 PC pixels in both x and y . So, to compensate for the systematic drift, the first and last F555W PC1 frames in this group of four were shifted by small amounts, using linear interpolation, before being combined with the other two frames. However, since the equivalent offsets are a factor of two smaller for the WF frames, and since the WF data is less well sampled than that for the PC, no offsets were applied to the WF data before combining. Finally the $4 \times 800 \times 800$ arrays for each of the 4 master frames were split into separate 800×800 arrays and then multiplied by the appropriate geometric correction distortion frames as supplied by STScI. The vignetted regions at the edges of the frames ($0 \leq x, y \leq 100$ for the PC, $0 \leq x, y \leq 75$ for the WF frames) were then removed. A mosaic of the combined F555W image from the second set of observations is shown in Fig. 1; note the completely resolved and relatively uncrowded appearance of this dwarf galaxy, reminiscent of ground-based images of galactic dSph systems. We note also that there are no globular star clusters evident in this And I image. None have been found on ground-based images either (MK90, Caldwell *et al.* 1992), and so it seems likely that And I lacks such clusters. This result is not unexpected given that And I’s luminosity is ~ 2 magnitudes fainter than those of Fornax and Sagittarius, the two galactic dSphs that possess their own globular cluster systems.

Fig. 1.— A mosaic of the And I WFPC2 field made from the combination of 4 1800 sec F555W images. North is indicated by the direction of the arrow and East by the line. Both indicators are $10''$ in length.

Photometry was then carried out on each of the sixteen combined data frames (2 positions, 2 filters, 4 CCDs) in the same manner. First, the IRAF/DAOPHOT routine *daofind* was used to find images on the frames. It was found that provided the threshold was kept reasonably high ($\sim 5\sigma$, where σ is the standard deviation of the background), the number of spurious objects

found was minimized. Aperture photometry was then carried out using the *daofind* coordinate list as input. For the PC1 frames the measurement aperture was 2.5 pixels in radius and the annulus in which the sky was determined had inner and outer radii of 6 and 16 pixels, respectively. For the WF frames the measurement aperture was 2.0 pixels in radius and the sky annulus lay between radii of 5 and 15 pixels. These measurement apertures are small enough to maximize the signal-to-noise ratio for faint stars but are not so small that centering uncertainty or variations in the PSF within the aperture across the frame are significant. No redetermination of the image centers was performed and, in all cases, the sky value was determined from the mode of the pixel intensity distribution within the sky annulus.

The first step in the subsequent processing was to compare the aperture magnitudes for the brighter stars on the two F555W frames and on the two F450W frames for each CCD. For the F450W frames the agreement is excellent: the mean values of the differences between the two measures being (0.004, 0.005, 0.001 and -0.001) with standard deviations of (0.034, 0.050, 0.038, 0.039) for (49, 119, 76 and 110) brighter stars on the (PC1, WF2, WF3, WF4) frames, respectively. As a result, the two sets of magnitudes were averaged for the stars in common, with the stars detected on only one frame or the other not retained. This process removes any remaining spurious images, such as “hot” (high dark current) pixels that do not follow the coordinate offsets between the real stars. For the two sets of F555W magnitudes, the corresponding magnitude differences (in the sense $set_1 - set_2$), standard deviations and sample sizes are (-0.039, -0.034, -0.040, -0.031), (0.025, 0.036, 0.035, 0.036) and (35, 96, 63, 90), respectively, for the (PC1, WF2, WF3, WF4) frames. There is clearly a systematic offset in the magnitudes here which we attribute to signal loss occurring during the combination process for the individual frames from the second F555W data set, the set during which the spacecraft drifted. Consequently, we have applied these mean offsets to the set_2 magnitudes before combining them with the magnitudes from set_1 . Again only stars measured on both frames were retained.

The next step requires the determination of the aperture corrections to convert the small measurement aperture magnitudes to magnitudes on the WFPC2 system (Holtzman *et al.* 1995b, hereafter H95b), which is based on standard apertures of $0.5''$ radius. These

aperture corrections are no doubt position dependant within each of the 4 CCD fields, but we lack the numerous bright high S/N stars needed to define well this spatial variation. We have therefore proceeded as follows. For the PC we first calculated aperture corrections for the dozen or so bright uncrowded stars for which such a determination was reasonably precise. Then we used the *Tiny Tim* PSF simulation package (Version 4.0b; Krist & Hasan 1993, Krist 1994) to calculate synthetic PSFs at the locations of these stars. These synthetic data frames were then measured in exactly the same way as the real stars and the resulting aperture corrections compared with the determinations from the real data. The agreement was quite satisfactory (average mean differences less than 0.01 mag) so we then used the *Tiny Tim* package to calculate, for each filter, a 64×64 grid of synthetic PSFs. This grid was then converted into a grid of aperture corrections and the small aperture photometry then corrected to the standard aperture size by interpolating in this grid.

For the WF CCDs however, this process was not as satisfactory. The *Tiny Tim* PSFs gave aperture corrections that were typically 0.05 mag larger than those calculated from the stars themselves, indicating that the real data is more centrally condensed than the model PSFs. We therefore decided to adopt a single aperture correction for each WF filter and CCD combination, thereby averaging over any spatial variation. These mean aperture corrections were determined from typically ten bright uncrowded stars on each frame with, at least for F450W, the values from the two datasets being averaged (the sets of stars used on each frame were generally not identical). Based on the *Tiny Tim* simulations, we expect that, for approximately the central two-thirds of the frame area, the adopted mean aperture corrections will be satisfactory. Outside this region, and particularly in the corners, the adopted aperture corrections will be underestimates (i.e. the true magnitude will be brighter) by up to perhaps a few hundredths of a magnitude at most. We note however, that this failure to account fully for the spatial variation in the aperture corrections on the WF frames will have only a second order effect on the colors of the stars since, based on the *Tiny Tim* modelling, the spatial variation is not a strong function of wavelength.

After application of the aperture corrections we can then employ the zeropoints and gain factors of H95b to place the photometry on the WFPC2 sys-

tem. One further correction needs to be applied however, and that is the correction for charge transfer effects (H95b). For the WF frames, we used the correction recommended in H95b, a simple linear ramp correction amounting to an increase in brightness of 0.04 mag for the stars at the highest y values. Note again that since this ramp was applied to both the F450W and F555W magnitudes, the colors of the stars are unaffected. For the PC however, plots of color-magnitude diagrams for different y -sections of the frame, after the application of a 0.04 mag/800 pixels ramp to both the F450W and F555W magnitudes, showed a distinct redward shift in the principal sequences with increasing y coordinate. We interpreted this result as indicating that a 0.04 mag/800 pixels ramp was inadequate for the F450W PC data, which has a background of only about $7e^-$ on the individual PC1 frames. A ramp of 0.10 mag/800 pixels was necessary to remove this effect. At this stage we now have fully corrected F450W and F555W magnitudes; all that remains is to combine the lists to produce F450W–F555W colors. As was the case for the magnitudes, only those stars that are found in both lists were retained, so that in effect, a star has to have been measured on all four frames (2 filters, 2 pointings) to be included on the final lists.

Since we are primarily interested in the morphology of the And I color-magnitude diagram, we can afford to edit the photometry lists to remove stars that may have larger than average errors. The principal source of additional error will be that which arises from image crowding. Although these frames are by no means crowded, there are still clearly instances where the light in the measurement aperture for one star is contaminated by light from a near neighbor. Accordingly, we removed from the photometry lists any star whose center lay within 5 (WF) or 9 (PC) pixels of the center of its nearest neighbor. These radii, which reduce the lists by about 15%, were chosen as the best compromise between maximizing the number of stars retained and reducing the scatter in the color-magnitude diagrams. Stars that lay near overexposed bright stars or on the mottled background of the few extended background galaxies were also removed at this stage. Finally, the stars remaining were visually inspected on the set_2 F555W combined frame. This led to the removal of a few additional “stars”, most of which were reclassified as marginally resolved background galaxies.

The final color-magnitude diagrams (hereafter cmds),

containing (256, 1074, 952 and 1226) stars brighter than $F555W = 26.7$, are shown in the panels of Fig. 2 for the (PC1, WF2, WF3 and WF4) data, respectively. There are clearly no obvious systematic differences between these 4 cmds. Moreover, calculations of mean colors and magnitudes at various places in the cmds indicate that any relative zeropoint differences between the four sets of data are at the ± 0.01 mag level at worst. We have therefore combined the data from the individual CCDs into a single color-magnitude diagram for Andromeda I containing 3508 stars. This diagram is shown in Fig. 3. Fig. 4 shows the equivalent V, B–V cmd which results from applying the transformation equations given in H95b to the data of Fig. 3.

Before discussing the astrophysical results that flow from Fig. 3, we turn first to a brief discussion of the *photometric* errors in these data. These errors are those that arise from the small aperture measurement process, as distinct from the systematic errors that arise from the uncertainty in the aperture corrections, in the zeropoint calibration, in the ramp correction, and so on. The photometric errors can be readily investigated by making use of the two sets of data we have available. For the stars in Fig. 3 then, we returned to the photometry lists for the two separate pointings and compared the magnitudes and colors. The results of this comparison are given in Table 1 where we have tabulated the average error in the mean of two measures (either magnitude or color) for the listed magnitude bins. Three points are worth making in connection with this table. First, at the fainter magnitudes ($F555W, F450W \gtrsim 26.0$) where the errors are relatively large, the mean errors in the magnitudes found from comparing the independent measures closely approximate the errors expected on the basis of the photon statistics alone. In other words, for uncrowded faint stars, the WFPC2 system is producing photon statistics limited data as is usually the case with ground-based CCD cameras. However, at the brighter magnitudes, this does not seem to be the case. For the brighter stars the photon statistics errors are below 0.01 mag yet on the basis of the frame-to-frame comparison, the decrease in the errors with increasing brightness flattens out and does not go below ~ 0.02 mag. This limit is probably the result of a number of inherent effects in the flat-fielding, dark subtraction and individual frame combination processes. Fortunately, the existence of such a limit does not compromise our data in any

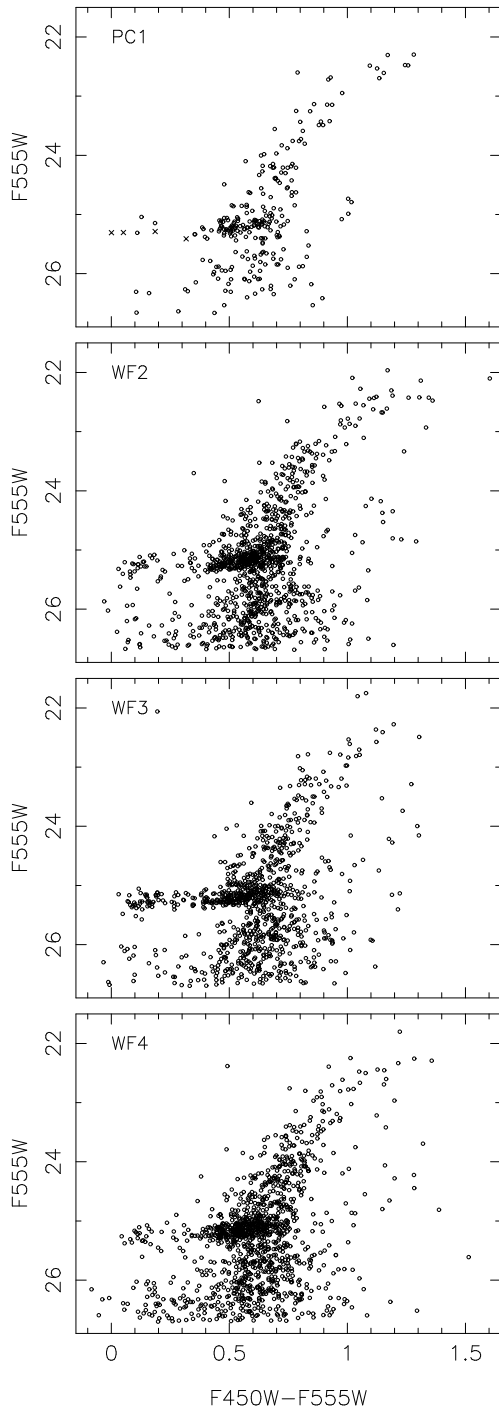


Fig. 2.— The And I color-magnitude diagrams, in the HST instrumental system, derived from the data for each WFPC2 CCD. The panels are labeled with the CCD identification. In the panel for the PC1 chip, the four RR Lyrae variables found in the PC1 data are plotted as \times -symbols.

way. Finally, we note that for the majority of stars, $\sigma_{F450W-F555W}^2 \lesssim \sigma_{F450W}^2 + \sigma_{F555W}^2$ as might be expected when the errors are not determined simply by photon statistics.

TABLE 1. Photometric Errors.

F555W	Mean Error in F555W	Mean Error in F450W-F555W	F450W	Mean Error in F450W
21.5–23.0	0.018	0.016	22.0–24.4	0.018
23.0–24.0	0.017	0.023	24.4–24.9	0.023
24.0–24.5	0.020	0.031	24.9–25.4	0.031
24.5–25.0	0.033	0.047	25.4–25.8	0.044
25.0–25.4	0.036	0.056	25.8–26.2	0.055
25.4–25.8	0.048	0.083	26.2–26.6	0.080
25.8–26.1	0.058	0.091	26.6–26.9	0.099
26.1–26.4	0.071	0.128	26.9–27.2	0.118
26.4–26.7	0.083	0.155

3. Results

In this section we will discuss the results that can be inferred from the And I cmd shown in Fig. 3, and its equivalent in the standard (V, B–V) system (Fig. 4). In this process we will first emphasize those results, such as the morphology of the horizontal branch, that do not depend on the photometric calibration of the cmd. Then we will move to those, such as the distance of And I, that depend primarily on the calibration of the F555W photometry and its transformation to V magnitudes. Finally, we will discuss quantities, such as the mean abundance of And I, which depend on the calibration of both the F450W and F555W magnitudes as well as on their transformation to standard B and V magnitudes. As we shall see, the F450W to B transformation is less well established than that of F555W to V.

3.1. Color-Magnitude Diagrams of And I

The morphology of the color-magnitude diagram shown in Fig. 3 is instantly recognizable as that of a basically old stellar population. A red giant branch that terminates at $F555W \approx 22.3$ and $F450W-F555W \approx 1.3$ is visible, and there is a dominant red horizontal branch at $V \approx 25.2$. A less well populated blue horizontal branch is also present. Stars evolving away from the red HB towards the asymptotic giant branch are evident to the blue of the giant branch for $V \gtrsim 24$. The three stars well to the blue of the giant branch with $F555W \approx 22.0$, $F450W-F555W \approx 0.2$ through

$F555W \approx 22.5$, $F450W-F555W \approx 0.6$ may be post-AGB stars. At all magnitudes a small number of stars are visible well to the red of the giant branch. In addition, there is a small population of faint ($F555W \gtrsim 26.0$), blue ($F450W-F555W \lesssim 0.25$) stars.

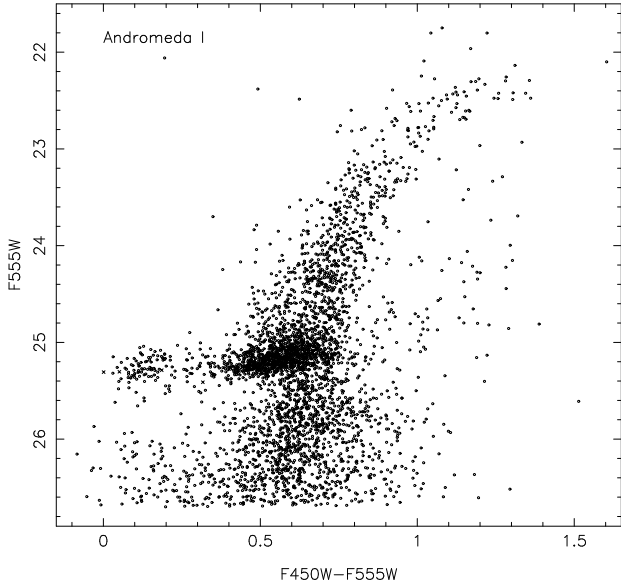


Fig. 3.— The combined Andromeda I color-magnitude diagram in the HST instrumental system. The dominant red horizontal branch morphology for this dSph galaxy is particularly striking. The 4 RR Lyrae variables found in the PC1 data are again shown as \times -symbols.

Before discussing these And I populations in more detail however, it is first necessary to consider the likely number of contaminating objects in Fig. 3 (and Fig. 4). Such objects can come from one of three components: foreground galactic stars, stars in the halo of M31, and unresolved background galaxies. Considering galactic foreground stars first, the model predictions of Ratnatunga & Bahcall (1985) suggest ~ 14 galactic foreground stars should be found in Fig. 4 with $B-V \geq 1.3$ and $23 \leq V \leq 25$. In Fig. 4, counting only the stars that are considerably redder and fainter than the 47 Tuc giant branch (see Fig. 8), there are ~ 30 to 35 stars in this color and magnitude interval. Given the uncertainties in the Ratnatunga & Bahcall model, and the fact that some of these “stars” may be unresolved galaxies, the agreement between the observed and predicted numbers is acceptable. Consequently, we can use the model prediction that bluer stars are much rarer at these magnitudes to conclude

that there are few, if any, galactic foreground stars with $B-V \lesssim 1.3$ in Fig. 4 at any magnitude. Thus the And I giant and horizontal branches are unaffected by foreground contamination.

To estimate the contribution of M31 halo stars to Figs. 3 and 4, we have proceeded as follows. And I lies some 3.3° from the center of M31 at a position angle of $\sim 135^\circ$ relative to the M31 major axis. The data of Pritchett & van den Bergh (1994) then suggest that the halo of M31 has a surface brightness at this location of perhaps 29.5 V mag/arcsec 2 , though the uncertainty in this number is large ($\sim \pm 1$ mag). On the other hand, using the surface brightness data of Caldwell *et al.* (1992), the average And I surface brightness over the region contained on the WFPC2 images is approximately 25.4 V mag/arcsec 2 . Then, under the reasonable assumption of similar stellar populations, the ratio of these two surface brightnesses predicts that And I stars should outnumber M31 halo stars by about 45 to 1, indicating a minor degree of contamination. We can attempt to verify this estimate by making use of the results of Durrell *et al.* (1994, see also Mould & Kristian 1986). These authors indicate that the mean abundance of the M31 halo is similar to that of the galactic globular cluster 47 Tuc, though there is a significant spread to higher and lower abundances. In Fig. 4 there are approximately 30 stars with $23 \leq V \leq 25$ that scatter about, and to the red of, the 47 Tuc giant branch (see Fig. 8) and which could reasonably be ascribed to the M31 halo, rather than to And I. After allowing for the M31 halo abundance spread (Durrell *et al.* 1994), this suggests that perhaps there are a total of ~ 40 M31 halo stars with $23 \leq V \leq 25$ in Fig. 4. The surface brightness scaling on the other hand would predict ~ 20 M31 halo stars in the same magnitude interval. Thus, as found for the galactic foreground stars, the “observed” number is higher than the predicted number, but we are not seriously concerned with this discrepancy. Even if the higher figure is valid, the comparative lack of metal-poor M31 halo giants (Durrell *et al.* 1994) ensures that the degree of contamination of the And I giant branch by (metal-poor) M31 halo stars is too small to affect any of the results.

As regards the numbers of unresolved background galaxies, the uncertainties in the actual contributions of the galactic foreground and M31 halo stars make it difficult to place any meaningful constraints. We note only that the results of Casertano *et al.* (1995), for example, indicate that E galaxies become smaller and

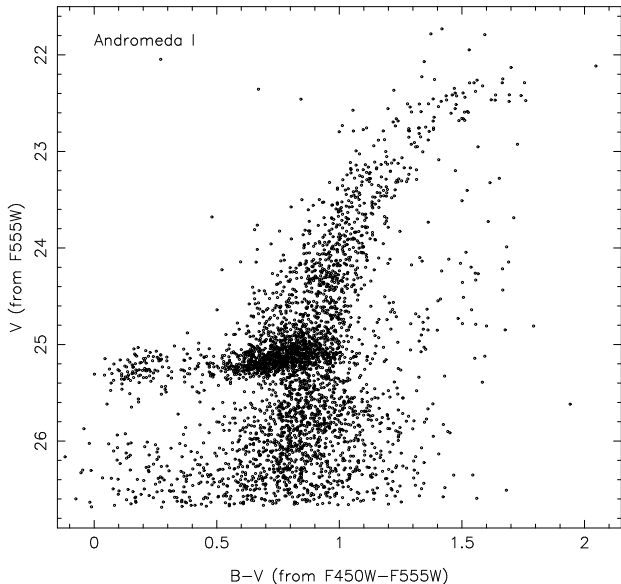


Fig. 4.— The combined Andromeda I color-magnitude diagram in the standard (V, B–V) system. The transformations applied to the HST instrumental system photometry are those of Holtzman *et al.* (1995b).

redder with increasing apparent magnitude. Thus while any unresolved background galaxies in our data may contribute to the “stars” that lie to the right of the And I giant branch in Fig. 4, it is unlikely that they will be a major contaminant of the And I giant and horizontal branches.

3.1.1. The Horizontal Branch Morphology

It is immediately apparent from Figs. 3 and 4 that the morphology of the horizontal branch in And I is dominated by red HB stars. Indeed, the red end of the HB is not clearly distinguishable from the blue edge of the red giant branch, as is usually the case in color-magnitude diagrams for old stellar populations. We believe this effect results from the combination of a number of factors. First, as indicated in Table 1, the photometric errors in the colors at the magnitude of the HB are approximately ± 0.06 mag. Thus an intrinsically narrow color width on the red HB would be broadened to an observed F450W–F555W color range of perhaps 0.24 mag. Second, the relatively small difference in effective wavelength between the F450W and F555W filters means that for a given effective temperature difference between a red HB star and a

red giant at the same magnitude, the color difference F450W–F555W will be smaller than it would be in, for example, the standard B–V system. Third, as we will argue below, there is an intrinsic color width to the And I red giant branch which is probably the result of an internal abundance range. Consequently, metal-richer red HB stars will lie closer in color to the metal-poorer red giants than would be the case for a single abundance population. An age range could also play a role here since the HB is redder and the giant branch somewhat bluer in a younger population (e.g. Sarajedini *et al.* 1995). Consequently, in conjunction with any real effective temperature spread among the And I red HB stars, these factors will combine to blur the distinction between red HB and red giant branch stars at the level of the horizontal branch. Nevertheless, it is apparent from Figs. 2 and 3 that the number of stars at the magnitude of the horizontal branch begins to decrease for colors redder than F450W–F555W ≈ 0.6 mag. We will therefore take this color as a reasonable estimate of the color blueward of which core helium burning stars dominate.

We can then quantify the HB morphology of And I as follows. Define b as the number of stars with $25.0 \leq F555W \leq 25.5$ and $0.0 \leq F450W-F555W \leq 0.25$ and r as the number of stars in the same magnitude interval but with $0.35 \leq F450W-F555W \leq 0.60$ mag. We can then calculate a HB morphology index $i = b/(b+r)$. This index⁴ (*cf.* Mironov 1973) ranges from zero for a pure red HB to unity for a pure blue HB. From the data of Fig. 3, this index has a value $i = 0.13 \pm 0.01$ for And I, where the error has been calculated assuming that both b and r are subject to Poissonian statistics.

How then are we to interpret this index? As we shall see in Sect. 3.3, the mean abundance of And I is $[\text{Fe}/\text{H}] = -1.45 \pm 0.2$ dex. At this abundance, the cmds of galactic globular clusters which follow the (HB morphology, $[\text{Fe}/\text{H}]$) relation defined by the majority of such clusters, have relatively many more blue HB stars and many fewer red HB stars than does And I. For example, the galactic globular cluster M5, which lies on the (HB morphology, $[\text{Fe}/\text{H}]$) relation for the inner-halo (the majority of clusters) in Lee *et al.* (1994), and for which $[\text{Fe}/\text{H}] = -1.40$ (Armandroff

⁴We cannot use the now common HB morphology index $(B-R)/(B+V+R)$, where B, V and R are the numbers of blue, variable and red HB stars, respectively, because we have not yet identified all the variables in the And I cmd shown in Fig. 3.

1989), has $i \approx 0.74$ using the cmd of Buonanno *et al.* (1981). In this sense we can then say that *And I shows the second parameter effect* in the same way as do many of the galactic dSph systems. Indeed our data for And I, as plotted in Fig. 4, bears many similarities to the ground-based cmd of Demers & Irwin (1993) for the galactic dSph companion Leo II. This dSph has a somewhat lower mean abundance than And I ($[\text{Fe}/\text{H}] = -1.9$, Demers & Irwin 1993; -1.9 ± 0.2 , Suntzeff *et al.* 1986; -1.60 ± 0.25 , Mighell & Rich 1996) but it also shows a predominately red HB. Demers & Irwin give $(B-R)/(B+V+R) = -0.68$ for Leo II from which we infer $i \approx 0.15$, a value similar to that found here for And I. Demers & Irwin (1993) also note that there is no obvious break between the red edge of the HB and the red giant branch in their ground-based cmd. However, in the Leo II cmds of Mighell & Rich (1996), which are derived from WFPC2 F555W and F814W observations and which are considerably more precise than the Demers & Irwin (1993) ground-based data, the red edge of the HB is separated by ~ 0.1 in $V-I$ from the red giant branch.

The horizontal branch in Figs. 3 and 4 does not, however, consist solely of red horizontal branch stars. Instead it extends to quite blue colors and this suggests that a search for RR Lyrae variables among the bluer HB stars could prove fruitful. As noted in Sect. 2, the F450W observations consist of two sets of six 1800 sec exposures separated by an interval of approximately 5.3 days. Within each set, the exposures are spaced by the HST orbital period of ~ 96 min so that the total interval covered by each F450W set of observations is ~ 0.4 day. These intervals, while not ideal, are adequate to search for RR Lyrae variables, since such stars have periods of $\lesssim 0.7$ day. Consequently, in order to carry out an initial reconnaissance for variable stars on the horizontal branch in And I, we have investigated the variability characteristics of the 14 stars on the PC frame with $25.0 \leq F555W \leq 25.5$ and $F450W - F555W \leq 0.43$ ($B-V \approx 0.6$).

A number of points have to be taken into account when assessing the results of this process. First, the individual data frames are, of course, not free of cosmic-ray contamination. As a result, although the aperture photometry was carried out in the same fashion as for the combined frame (using the centers determined from the combined frame), each variable candidate had to be inspected visually on each frame to be certain that the aperture measurement was not affected by cosmic rays. Typically two of the six possi-

ble measurements from each set of F450W frames had to be discarded. Second, the individual photometric errors are in the range (1σ) $\sim 0.10 - 0.15$ mag. Therefore, when considering the set of (at most twelve) individual F450W magnitudes, variations had to exceed $0.4 - 0.5$ mag before they were taken as an indication of possible intrinsic variability. Hence we are not likely to detect any variables whose amplitudes are less than these values. For the same reason we are likely to miss any variable whose maximum occurred outside the two ~ 0.4 day observing windows. However, despite these complications, it was quite obvious that four of the 14 candidates varied with F450W (full) amplitudes ranging from ~ 0.6 mag to ~ 1.2 mag. These stars are identified in the PC1 c-m diagram of Fig. 2 by the use of a \times -symbol. The colors of these variables, from the final combined frame photometry, are all significantly bluer than the color cutoff used to define the candidates, so that, subject to the caveats given above, it is unlikely that we have missed many additional variables.

For these four stars we have used the individual magnitudes and the mid-exposure times as input into the Phase Dispersion Minimization (PDM) routine within IRAF, in order to generate estimates of their periods. The five day gap between the two sets of observations necessarily introduces some ambiguity into this process and as a result, we have resorted to use of the period-amplitude relations exhibited by RR Lyrae stars in the galactic dSph systems (e.g. Kaluzny *et al.* 1995 and references therein) to aid in identifying the appropriate number of cycles between the two datasets. Photometry of these stars from the F555W observations (3×1800 sec and 4×1800 sec preceding the corresponding F450W observations) was also employed to constrain the range of possible periods.

The results of this process are shown in Fig. 5 where we present light curves for the four variables. Two of the stars are evidently type ab RR Lyrae stars while the other two are type c variables. The periods given for these stars are accurate only to a few digits in the third significant figure and the phase is relative to the mid-exposure time of the first 1800 sec F450W exposure. With such a small sample it is impossible to draw any firm conclusions from the properties of these And I RR Lyrae variables. Nevertheless, we note that the relative number of RRc and R Rab stars discovered here in the PC data is not incompatible with that seen in the Sculptor dSph: Kaluzny *et al.* (1995) have found 89 type c and 134 type ab variables

in this system. We also note that, given the relative areas of the PC and WF frames, a total population of perhaps 50 to 60 And I variables should be present in the entire dataset. The characteristics of these stars will be the subject of a subsequent paper.

3.1.2. Radial Gradients?

Color-magnitude diagram studies of the galactic dSph companions are generally limited, by the large apparent size of these galaxies, to regions well within the core radius. This restriction necessarily constrains any search for radial gradients whose presence, or confirmed absence, would provide important clues to the formation of dSph systems. For And I, where the core radius⁵ as determined from the surface photometry study of Caldwell *et al.* (1992), is $95 \pm 5''$, there is sufficient radial coverage in the WFPC2 data to look somewhat beyond the galaxy's core. We have therefore sought to identify any radial trends present in the characteristics of the cmds shown in Figs. 3 and 4. As a first step, it is necessary to transform the “local” x and y coordinates from the photometry for each WFPC2 CCD to a single global system. At the level of precision required here, it is not necessary to allow for the slight rotations and misalignment of the CCDs nor for the minor scale changes induced by the camera distortions. Instead a simple global system was adopted which has x and y axes parallel to those of the PC1 data and which has its origin at the camera apex. The original coordinates from the WF CCD photometry were then flipped and changed in sign as appropriate and those from the PC1 photometry multiplied by the relative PC to WF scale factor of 0.457 (H95a). Then, since the center of And I (also determined from the surface photometry of Caldwell *et al.* 1992) was centered on the center of the PC1 field, it is straightforward to generate cmds similar to those of Figs. 3 and 4 for different distances from the galaxy's center. Caldwell *et al.* (1992) have also shown that And I is circularly symmetric so no allowance for ellipticity is necessary.

We have first investigated the radial dependence of the mean color of the giant branch at a number

⁵Throughout this paper the term “core radius” is taken to mean the radius at which the projected surface brightness profile reaches one-half of its central value. As a result of the low central concentrations of dSph galaxies, the core radius defined in this way is generally somewhat smaller than the “core radius” parameter derived from a King (1966) model fit to the surface brightness profile data.

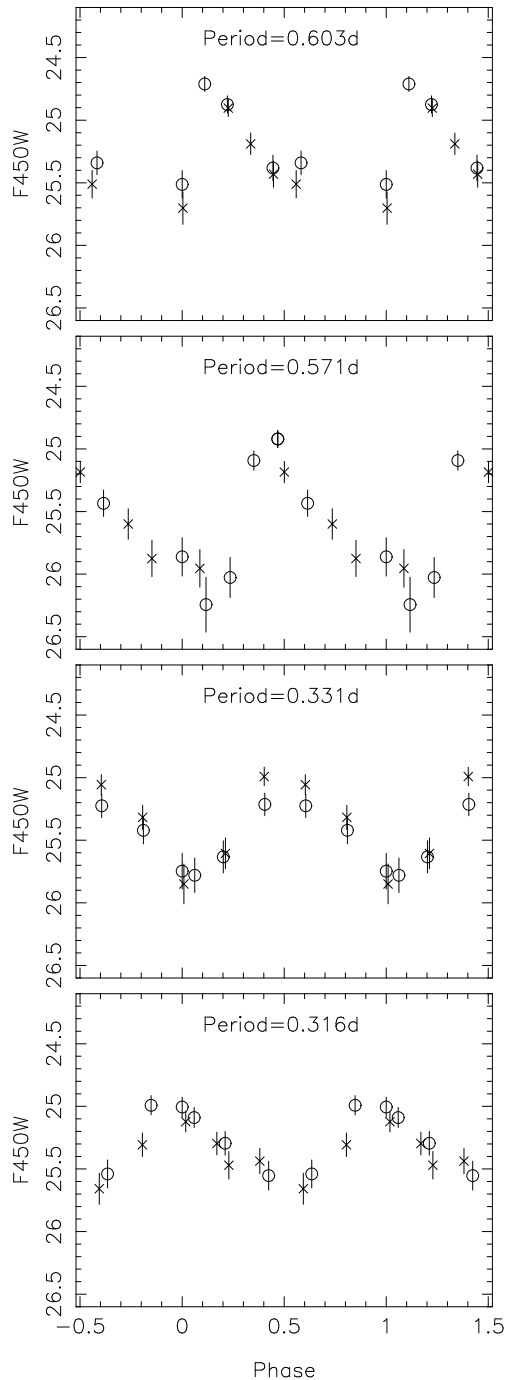


Fig. 5.— F450W light curves for the 4 RR Lyrae variables found in the PC1 photometry. Two cycles are plotted for each variable with open circles and \times -symbols representing magnitudes from the two sets of F450W observations. The error bars are those from the photon statistics. The adopted periods are given in each panel.

of different luminosities. This will provide limits on any radial variation in the mean abundance of And I's dominant stellar population. No evidence for any change with distance from the galaxy's center was found. For example, if we consider just two samples, namely the stars inside and outside a radius of 900 pixels (i.e. $\sim 90''$ or approximately 1 core radius), then the mean B–V colors for stars inside the dividing radius are 0.85 ± 0.01 (std error of the mean) for $25.5 \leq V \leq 25.7$ and 1.15 ± 0.02 for stars with $23.1 \leq V \leq 23.3$. For the stars outside the dividing radius, the corresponding mean colors for the same magnitude intervals are 0.87 ± 0.02 and 1.16 ± 0.03 , respectively. This lack of any significant difference in mean color is found regardless of the radial binning chosen or of the luminosity range considered. Anticipating the abundance calibration discussed in Sect. 3.3 below, these results imply an upper limit of ~ 0.2 dex for any change in the And I *mean* abundance over a radial distance from the center to ~ 1.2 core radii. This result is consistent with those of Caldwell *et al.* (1992) who found that And I's integrated B–V color is constant (at the $\pm 1\sigma = 0.02$ mag level) inside a radius of $\sim 120''$ or ~ 1.3 core radii. We emphasize though that this result applies to the dominant stellar population in And I; an abundance gradient could still occur in any minor stellar population component present.

The second quantity we have investigated for any radial dependence is the horizontal branch morphology index $i = b/(b+r)$. Unlike the mean giant branch color where any radial change reflects changes in the properties of the dominant stellar population, the HB morphology index is sensitive to changes in the relative numbers of blue HB stars, which are only a *minor* component (recall $i = 0.13 \pm 0.01$ for the complete sample). We first split the total sample radially into four subsamples each containing roughly equal numbers of stars and then computed the HB morphology indices. Intriguingly, the value of i for the outermost radial bin was substantially larger (i.e. relatively more blue HB stars) than for the other more centrally located samples. This led us to conduct a number of experiments with different radial selections. From these we have ascertained that within approximately one core radius⁶ there is no radial variation in the HB morphology index. However, outside the core radius,

there are indeed relatively more blue HB stars. This is illustrated in Fig. 6 which shows cmds for the regions with $r \leq 900$ pix (i.e. $\sim 90''$, upper panel) and $r \geq 900$ pix (lower panel). The average distance from the center of And I in these cmds is $\sim 60''$ for the stars in the inner sample and $\sim 100''$ for the outer sample. It is apparent from these cmds that the outer region has a higher proportion of blue HB stars. Quantitatively, we have $i = 0.109 \pm 0.013$ for the inner region ($b = 64$, $r = 523$) and $i = 0.195 \pm 0.031$ for the outer region ($b = 31$, $r = 128$). In both cases the error is calculated assuming Poissonian statistics.

How significant is this difference? In comparing proportions, as we are doing here, the relevant statistic (e.g. Arnold 1990) is:

$$T_2 = \frac{\hat{p}_1 - \hat{p}_2}{[\hat{p}(1 - \hat{p})(n_1^{-1} + n_2^{-1})]^{1/2}}$$

where, in our case, \hat{p}_1 and \hat{p}_2 are the values of i for the inner and outer regions, respectively, n_1 and n_2 are the total numbers of blue and red HB stars in each region, and \hat{p} is the value of i for the entire (inner + outer) sample. Inserting the numbers into this equation then yields $T_2 = 2.88$ which, since the statistic has a normal distribution with mean zero and unit variance, implies that there is a less than 1% chance that the two proportions are drawn from the same underlying population. Alternatively, since the outer group is approximately 30% of the inner group in size, we can run simulations in which 3 from every 10 stars in the inner group are selected and the value of the HB morphology index calculated. We find that for 120 independent samples of the same size as the outer data set, the *largest* value of i was 0.175, still notably less than the observed value of i for the outer group. Thus, once again, it appears that there is a less than 1% probability that the observed HB morphology difference arises by chance.

We conclude therefore that from inside to outside approximately one core radius, the relative number of blue HB stars increases by somewhat less than a factor of two. In other words, it appears that the blue HB population of And I is more widely dispersed than the red HB population. There does not, however, appear to be any other difference between the two groups of HB stars. For example, the mean F555W magnitudes of the red HB stars are 25.21 and 25.22 for the inner and outer regions, respectively, while for the blue HB stars, the corresponding values are 25.25 and 25.27. The mean F450W–F555W colors are also

⁶Since the core radius was determined from surface photometry, it corresponds to that of the dominant stellar population, i.e. the population that generates principally red HB stars.

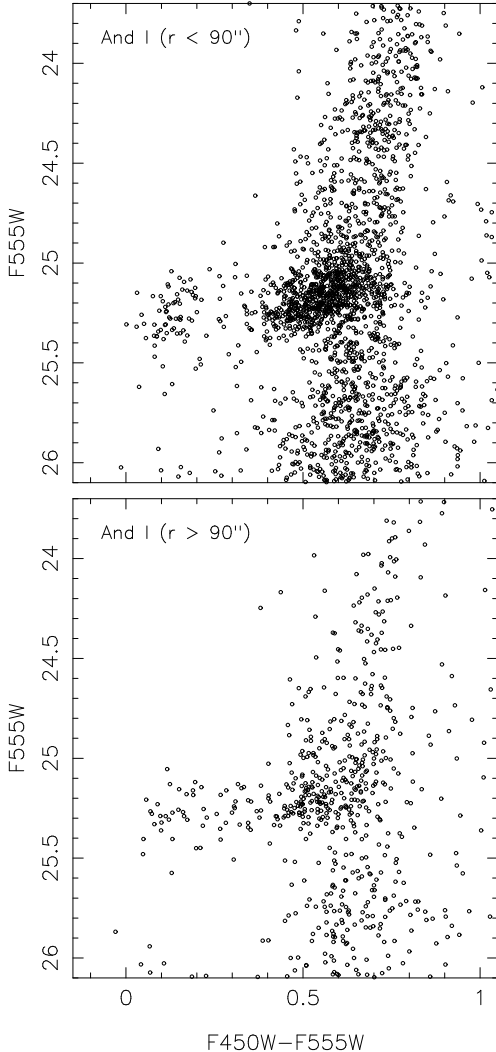


Fig. 6.— And I color-magnitude diagrams emphasizing the change in horizontal branch morphology with distance from the center of this dSph. The upper panel is for stars within $90''$ of the center, while the lower panel is for stars at radial distances of more than $90''$. The relatively larger fraction of blue HB stars in the lower panel is evident.

similar: 0.13 and 0.52 for the inner blue and red HB stars, and 0.14 and 0.51 for the HB stars in the outer sample.

What change in fundamental characteristics of the stellar population of And I could contribute to this observed gradient in HB morphology? Ignoring other possible (but not easily quantified) causes such as variable mass-loss rates, etc, inspection of the HB calculations of Lee *et al.* (1994) shows that first, at a mean abundance near $[\text{Fe}/\text{H}] = -1.5$, a decrease in age of 3 to 4 Gyr is required to change a blue HB into a red one, and second, at an age of ~ 12 to 15 Gyr, an increase in abundance of perhaps 0.6 dex is required for the same effect. Suppose then that the HB of And I is made up of two components which differ in age or abundance by these amounts. In the inner region the (younger or more metal-rich) red HB population comprises $\sim 86\%$ of the total while in the outer region it is somewhat less dominant, contributing $\sim 75\%$ of the total. Could we detect these age or abundance changes via, for example, the effect on the mean giant branch color? If age is the distinguishing characteristic then the answer is a definite “no”; the lack of sensitivity of giant branch color to age combined with the small relative number of the “old” stars means that the predicted difference in giant branch color is negligible. If however, an abundance difference of ~ 0.6 dex is the distinguishing characteristic, then the approximate doubling in size of the contribution of the metal-poor component from the inner to the outer region would generate a change in the mean $B-V$ color of the upper giant branch of ~ 0.03 mag, with the color for the outer region being bluer. In fact no such color difference is seen in the actual data, though the small numbers of stars on the upper giant branch in the outer region limit the precision of this test. We cannot therefore easily identify the underlying cause of the HB morphology gradient; neither an abundance gradient nor a change in the mean age (or a combination of both) can be positively ruled out. Nevertheless, as we will see in Sect. 4, the existence of a 10 – 15% population that is 0.5 – 0.6 dex more metal-poor than the mean is unlikely given the relatively narrow intrinsic abundance distribution in this galaxy.

3.1.3. The Giant Branch Intrinsic Color Width

In their study of the upper \sim two magnitudes of the And I giant branch, MK90 pointed out that the observed color width in their cmd was considerably larger than that expected from their photomet-

ric errors. Thus an intrinsic color range was clearly present. By analogy with the galactic dSph systems, where intrinsic abundance spreads are well established (e.g. Suntzeff 1993), MK90 then concluded that the intrinsic color range on the And I giant branch was due to a spread in abundance; they estimated that more than the central two-thirds of the distribution was contained in the abundance interval $-2.0 \lesssim [\text{Fe}/\text{H}] \lesssim -1.0$.

We can also use our data to characterize this property of And I by investigating the giant branch color width at an appropriate luminosity. Ideally this luminosity would be below that of the horizontal branch where contamination by AGB stars is not a concern. However, at these fainter magnitudes, the relatively large size of the photometric errors as compared to the observed color width precludes reliable analysis. At brighter magnitudes, for example $24.5 \gtrsim F555\text{W} \gtrsim 23.5$, it is evident from Fig. 3 that stars evolving away from the red horizontal branch onto the AGB would compromise any analysis of the red giant branch color width. However, based on the c-m diagrams of galactic globular clusters, it does appear that the AGB eventually either terminates or merges into the red giant branch. Thus the stars at higher luminosities can be used to constrain the size of any intrinsic color width present. We have chosen to study the color width of the giant branch over the magnitude interval $23.5 \geq F555\text{W} \geq 22.7$ since at brighter magnitudes the giant branch turns over, becoming almost horizontal (*cf.* Fig. 3) making it difficult to easily interpret any color width. The faint magnitude limit is set to minimize the influence of AGB stars.

As a first step we fitted a low order polynomial to the stars in the magnitude interval $24.2 \geq F555\text{W} \geq 22.4$, excluding obvious outliers. Then for each star with $23.5 \geq F555\text{W} \geq 22.7$, we determined the residual in $F450\text{W}-F555\text{W}$ color from this mean giant branch at the $F555\text{W}$ magnitude of the star. The distribution of these residuals for the 105 stars considered And I giants is shown as a histogram in Fig. 7, together with the residuals for the outlier stars that were excluded from the determination of the mean giant branch. The distribution for the assumed And I stars appears to be reasonably uniform over a ~ 0.2 mag full range, but statistically the distribution is not significantly different from a gaussian. It can be characterized in a number of ways. For example, the standard deviation σ is 0.06 mag, the inter-quartile range is 0.09 mag and the central two-thirds of the

distribution is contained in a residual range of 0.14 mag. These values do not change substantially if the magnitude interval considered is altered by reasonable ($\sim 0.2 - 0.3$ mag) amounts. Similarly, if we divide the sample into two groups consisting of the stars inside and outside ~ 1 core radius, there is no evidence for any difference in the respective residual distributions.

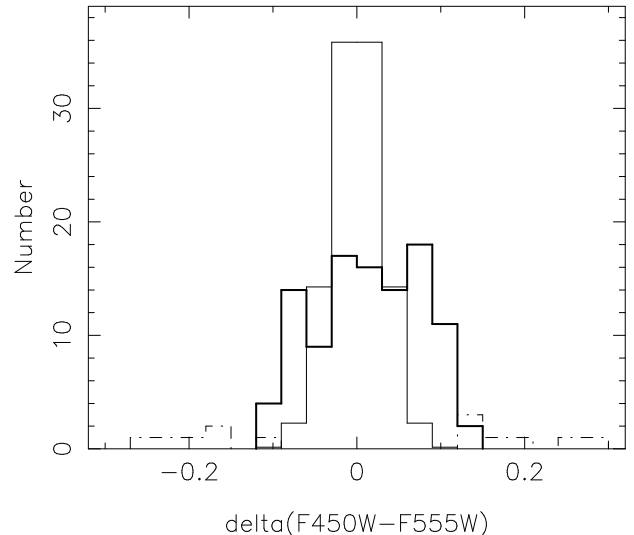


Fig. 7.— Histogram of $F450\text{W}-F555\text{W}$ residuals from the mean And I giant branch for the magnitude interval $22.7 \leq F555\text{W} \leq 23.5$. The thick solid line is for the stars considered likely members of And I while the dot-dash line is for those stars not considered And I members. The thin solid line is the distribution expected on the basis of the instrumental errors alone, if And I does not contain an internal abundance range.

As discussed above, the photometric errors for these data have been determined by comparing magnitudes and colors derived from the two independent sets of observations. For the magnitude interval considered here, we have $\sigma(F450\text{W}-F555\text{W}) \approx 0.02$ mag, which is considerably smaller than the observed standard deviation. A gaussian distribution with this σ and the same sample size is also plotted in Fig. 7 to emphasize the difference between the observed distribution and the distribution expected on the basis of the photometric errors alone. We emphasize that although errors in the calibration and in the adopted aperture corrections, for example, will affect the zeropoint of the observed colors, the parameters characterizing the distribution of residuals from the mean giant branch are unaltered by these systematic effects.

Hence we conclude that the spread in color on the And I giant branch implied by Fig. 7 is dominated by an intrinsic range in the colors of the And I stars (*cf.* MK90). We defer, however, to section 3.4 a discussion of the corresponding abundance range in And I.

3.1.4. A Population of Blue Stragglers?

In the lower left portion of Fig. 3 a small population of faint ($F555W \gtrsim 26.0$), blue ($F450W - F555W \lesssim 0.25$) stars is visible. At $F555W$ magnitudes between 26.0 and 26.4, the mean repeatability error in the $F450W - F555W$ colors is less than 0.15 mag. Thus it seems unlikely that all of these faint blue stars could result from 3 or 4σ errors in the photometry. We note though that incompleteness in the $F450W$ data, which begins to be significant at perhaps $F450W \approx 26.8$, means that we should not expect a symmetrical scatter in the $F450W - F555W$ colors about the mean giant branch ridge line at these magnitudes. For example, the relative lack of stars in Fig. 3 with $F555W \gtrsim 26.0$ and $F450W - F555W \gtrsim 1.0$ is probably a consequence of this effect. Nevertheless, the fact that the faint blue stars in Fig. 3, like all the stars plotted, have been detected and measured *on both frame pairs* suggests strongly that these stars do represent a *bona fide* And I population.

What then are these faint blue stars? There are two possibilities. First, the stars could be on or near the main sequence turnoff for an And I population with an age of perhaps 1.5 to 2.5 Gyr. However, although we cannot completely dismiss this possibility, we consider it unlikely since there is no other evidence to suggest the presence of an intermediate-age (age $\lesssim 10$ Gyr) population in this dSph. In particular, MK90 give 2σ upper limits of 10%, for the fraction of any And I population with ages between 0.5 and 3 Gyr and 20%, for a 3 to 10 Gyr population. Similarly, Armandroff *et al.* (1993), using the data of MK90, estimate a 3 to 10 Gyr population fraction in And I of $10 \pm 10\%$ while Armandroff (1994) reports that no luminous upper-AGB carbon stars have been detected in And I.

The alternative explanation for these faint blue stars is that they are *blue stragglers* similar to the brightest examples seen in galactic globular clusters and in some of the galactic dSph galaxies (e.g. Ursa Minor, Olszewski & Aaronson 1985). Inspection of Fig. 10 of Fusi Pecci *et al.* (1992) for example, supports this interpretation. In that figure, which shows

a c-m diagram for a composite sample of 425 blue stragglers in 21 galactic globular clusters, the brightest such stars have $(B-V)_0$ colors between -0.10 and 0.35 and absolute visual magnitudes between ~ 1.5 and 2.0 . Anticipating the results of the next section, these limits correspond to $-0.05 \lesssim B-V \lesssim 0.40$ and $26.2 \lesssim V \lesssim 26.7$ at And I. These values are consistent with the location of the And I faint blue stars in Fig. 4, though the brightest of the And I candidate blue stragglers, at $V \approx 26.0$ ($M_V \approx 1.3$), are about 0.2 mag brighter than the brightest of the galactic globular cluster blue stragglers. We do not, however, regard this as a serious concern. If, as discussed below, the predominantly red HB in And I indicates an age for the majority of the population that is younger than the galactic globular clusters, then the turnoff mass in And I will be correspondingly higher. This in turn will permit the formation of somewhat more massive, and therefore more luminous, blue straggler stars.

3.2. The Distance of And I

The reddening maps of Burstein & Heiles (1982) indicate $0.03 \leq E(B-V) \leq 0.06$ for And I; we adopt $E(B-V) = 0.04 \pm 0.02$ and thus $A_V = 3.2E(B-V) = 0.13 \pm 0.06$ mag. In Fig. 4, the 89 stars with $25.0 \leq V \leq 25.4$ and $0.0 \leq B-V \leq 0.35$ yield a mean magnitude for the horizontal branch of 25.25 ± 0.04 . The statistical uncertainty in this value is small (~ 0.01 mag) but we have adopted ± 0.02 mag as the error in the mean aperture corrections and ± 0.03 mag as the uncertainty in the adopted $F555W$ (V) magnitude zeropoint. Walker (1995, *priv. comm.*) has indicated that the V magnitude zeropoint appears stable at this level over a four month interval that encompasses the And I observations (see also, Ritchie 1995). To convert this V_{HB} value into a distance modulus for And I however, requires the adoption of a horizontal branch luminosity calibration. Such calibrations usually take the form $M_V(RR) = a[Fe/H] + b$ though the values of the coefficients a and b remain contentious. We follow Da Costa & Armandroff (1990) in adopting $a = 0.17$ and $b = 0.82$, which is the relation derived from the horizontal branch models of Lee, Demarque & Zinn (1990) for a helium abundance $Y = 0.23$. This calibration is also the basis of the distance scale that uses the I magnitude of the red giant branch tip in old stellar populations (Da Costa & Armandroff 1990; Lee, Freedman & Madore 1993a).

Adopting a mean abundance of $[Fe/H] = -1.45 \pm$

0.2 (see below), then yields $(m - M)_V = 24.68 \pm 0.05$ and $(m - M)_0 = 24.55 \pm 0.08$ for And I, corresponding to a distance of 810 ± 30 kpc. This distance agrees well with that given by MK90 (790 ± 60 kpc), which is based on the I magnitude of the And I giant branch tip but which uses a calibration that assumes $M_V(\text{RR}) = +0.6$ for all $[\text{Fe}/\text{H}] \leq -1.0$. Since, at the abundance of And I derived here, $M_V(\text{RR})$ on our adopted scale is very close to 0.6, no adjustment of the MK90 result is required.

To compare our distance to And I with that for M31 however, requires an M31 modulus that is on the same distance scale. There are two appropriate determinations. First, Pritchett & van den Bergh (1988) have determined the mean magnitudes of RR Lyrae stars in an M31 halo field. Adopting a mean abundance of $[\text{Fe}/\text{H}] \approx -1.0$ for these stars (Pritchett & van den Bergh 1988), then yields an M31 distance modulus $(m - M)_0 = 24.35 \pm 0.15$ on our adopted scale⁷. Second, Mould & Kristian (1986) give $I = 20.55 \pm 0.15$ mag for the apparent I magnitude of the red giant branch tip in their M31 halo field. Assuming a reddening of $E(\text{B}-\text{V}) = 0.08 \pm 0.02$ for this field and noting that $M_I(\text{RGB}_{\text{tip}}) \approx -4.05 \pm 0.10$ for old metal-poor red giants (Da Costa & Armandroff 1990), then yields $(m - M)_0 = 24.45 \pm 0.20$ for M31 on our adopted distance scale. Together these determinations suggest $(m - M)_0 = 24.40 \pm 0.13$ for M31 or a distance of 760 ± 45 kpc. Thus, on the basis of these data, And I is apparently some 50 ± 50 kpc beyond M31 along the line-of-sight.

The recent HST results of Ajhar *et al.* (1996) however, give a somewhat contradictory picture. Ajhar *et al.* (1996) give V_{HB} values for three globular clusters and two field regions in M31 based on WFPC2 images in the F555W and F814W filters. Considering first the two metal-poor globular clusters (K105 and K219) where no adjustment is necessary to convert V_{HB} to V_{RR} , and noting that we adopt a reddening $E(\text{B}-\text{V}) = 0.045 \pm 0.02$ for K219, the mean V_{HB} values of Ajhar *et al.* (1996) lead to distance moduli of 24.75 ± 0.08 and 24.65 ± 0.07 , respectively, on our adopted distance scale. The uncertainties are those given by Ajhar *et al.* (1996) for their $V_0(\text{HB})$ values. For the metal-rich cluster K58, we choose to adjust V_{HB} by the same amount as used by us for 47 Tuc

(0.15 mag) leading to a modulus of $(m - M)_0 = 24.55 \pm 0.11$ for this cluster. Together these three clusters then imply an M31 modulus on our adopted scale of 24.65 ± 0.1 corresponding to a distance of 850 ± 40 kpc. In this situation, And I is then apparently 40 ± 50 kpc in front of M31. The two field regions considered in Ajhar *et al.* (1996), which are near the clusters K58 and K108, are undoubtedly contaminated by a younger population from M31's outer disk. It is therefore not straightforward to convert the observed mean magnitude for the red horizontal branch (red clump?) to an equivalent V_{RR} . Nevertheless, the Ajhar *et al.* (1996) data for these fields, taking a V_{HB} to V_{RR} correction of 0.2 mag and assuming a mean abundance of $[\text{Fe}/\text{H}] \approx -0.3$ (Ajhar *et al.* 1996) also imply an M31 distance modulus of approximately 24.60 on our adopted scale.

Given these results then, it is apparent that we cannot at the moment precisely determine the relative line-of-sight distance between M31 and And I; a value of 0 ± 70 kpc would seem to be the best estimate. Clearly, an accurate determination of V_{HB} from a sizeable sample of M31 halo field blue horizontal branch and RR Lyrae stars would be the best way to reduce the uncertainty in this relative line-of-sight distance determination⁸.

At an M31 distance of between 760 and 850 kpc, the projected distance of And I from the center of M31 is ~ 45 kpc, so that, given the above results, And I lies at a true distance of between ~ 45 and ~ 85 kpc from the center of M31. The lower limit is considerably smaller than the galactocentric distances of the nearer dSph companions to the Galaxy, such as Ursa Minor ($R_{gc} \approx 70$ kpc), Draco and Sculptor (both $R_{gc} \approx 80$ kpc) though it does exceed the galactocentric distance of the Sagittarius system, which has R_{gc} of ~ 16 kpc. However, the Sgr dSph is clearly being strongly affected by the tidal field of the Galaxy while And I has a smooth undistorted surface brightness profile (Caldwell *et al.* 1992). This suggests a possible al-

⁷van den Bergh (1995) gives a mean V_0 of 25.04 for this same RR Lyrae sample, yielding $(m - M)_0 = 24.39$ on our adopted distance scale.

⁸In a recent preprint, Fusi Pecci *et al.* (1996) have reanalyzed the Ajhar *et al.* (1996) data, combining the results with similar data for an additional four M31 globular clusters. On our adopted scale, and with our adopted correction to V_{HB} for metal-rich red HB clusters (0.15 mag, *cf.* 0.08 mag in Fusi Pecci *et al.* 1996), the mean modulus for the eight clusters is $(m - M)_0 = 24.64 \pm 0.05$, corresponding to a distance of 850 ± 20 kpc. These values agree very well with those given by Ajhar *et al.* (1996), and again indicate that And I lies 40 ± 40 kpc in front of M31. Thus our adoption of 0 ± 70 kpc for the And I/M31 line of sight distance is unaltered by these new data.

ternative approach to estimating the true distance of And I from the center of M31.

The surface brightness profile of Caldwell *et al.* (1992) yields a “tidal” radius for And I of 2.8 ± 0.3 kpc from a King (1966) model fit. Further, Caldwell *et al.* (1992) also give a total integrated magnitude M_V of -11.7 for And I. If we then assume a mass-to-light ratio M/L_V of ~ 10 for And I (*cf.* Mateo *et al.* 1993, Fig. 8 and Peterson & Caldwell 1993, Fig. 2), we can then apply the relation of King (1962, equation 12) to generate predicted tidal radii for various assumed And I perigalactic distances. If we take a M31 mass of $5 \times 10^{11} M_\odot$, then for a perigalactic distance of 45 kpc, the predicted tidal radius is 1.3 kpc, a value more than a factor of two smaller than the observed limiting radius. For a perigalactic distance of 90 kpc however, the predicted tidal radius is ~ 2.5 kpc in better accord with the Caldwell *et al.* (1992) observations. Consequently, although there are obviously a number of uncertain factors in this analysis, such as the assumed M/L for And I, the mass of M31 and more significantly, whether the observed limiting radius of And I is actually set by M31’s tidal field (*cf.* Seitzer 1985), the results do suggest that the true distance of And I from the center of M31 is nearer the upper limit suggested above (i.e. $R \sim 85$ kpc) than the lower.

3.3. The Abundance of And I

The determination of an abundance estimate for And I from these data requires a comparison with the giant branches of galactic globular clusters of known abundance. Since there are no such giant branches available in the WFPC2 (F555W, F450W–F555W) system, we are forced to rely on the transformations listed by H95b to convert our data to the standard B,V system. The F555W filter is one of the primary photometric filters so that it is well calibrated (H95b). Similarly, the F555W to V transformation has only a small color dependence, so that we do not expect this transformation to introduce any significant uncertainties. On the other hand, the F450W filter is not one of the primary filters and its calibration is determined synthetically (H95b). This requires accurate modelling of the overall system response; H95b suggest an uncertainty of $\sim 2\%$ in this approach. Further, the transformation of the F450W–F555W colors to standard B–V is also based on a synthetic process, via the use of a library of stellar spectrophotometry (H95b). This library (e.g. Gunn & Stryker

1983) contains principally bright solar neighborhood dwarfs and giants of presumably approximately solar abundance. Thus, given the large color coefficients in the F450W–F555W to B–V transformation ($F450W-F555W \approx 0.71(B-V) + 0.036(B-V)^2$, H95b) its applicability to lower gravity metal-poor globular cluster giants is not clear-cut. We have therefore begun a program of observing standard globular clusters with ground-based telescopes using F450W and F555W (and standard B, V) filters together with a CCD whose response is similar to that of the WFPC2 devices. However, this program is not yet complete and so for the present we shall assume the applicability of the H95b transformation for F450W–F555W keeping in mind the possibility of both zeropoint and systematic effects.

In Fig. 8 we again present the And I photometry, transformed to the (V, B–V) system using the H95b transformations, together with the giant branches for the galactic globular clusters M68 (Walker 1994), M55 (Lee 1977), NGC 6752 (Cannon & Stobie 1973), NGC 362 (Harris 1982) and 47 Tuc (Hesser *et al.* 1987). The adopted reddenings, $V(HB)$ values and abundances of these clusters are given in Table 2. These giant branches were initially placed on the And I data using the $(M_V(HB), [Fe/H])$ relation described above, an apparent modulus $(m - M)_V = 24.68$ and a reddening $E(B-V) = 0.04$ mag. However, with this reddening, the agreement between the observations and the standard globular cluster giant branches was not satisfactory, particularly for the region of the And I cmd fainter than the horizontal branch. As is shown in the figure, a more satisfactory fit is achieved if the globular cluster giant branches are reddened by a further 0.05 mag in B–V, with no change in the V magnitudes. Given the uncertainty in the zeropoint of the F450W calibration and the uncertainty in the zeropoint of our photometry (e.g. $\sim \pm 0.02$ mag is the error in the adopted mean aperture corrections), this requirement for an additional color shift does not seem unreasonable⁹.

We can now proceed to derive an estimate for the mean abundance of And I; an estimate of the size of the abundance spread implied by the intrinsic color width discussed in Sect. 3.1.3 above will be derived in the next section. The mean abundance estima-

⁹We have recently acquired B, V CCD frames of And I using the WIYN telescope. When reduced, these data will clarify the situation regarding the zeropoints of the photometry shown in Figs. 4 and 8.

TABLE 2. Adopted Parameters for Standard Galactic Globular Clusters.

Cluster	[Fe/H]	V(HB)	E(B-V)
NGC 104 (47 Tuc)	-0.71	14.06	0.04
NGC 362	-1.28	15.43	0.04
NGC 6752	-1.54	13.75	0.04
NGC 6809 (M55)	-1.82	14.40	0.14
NGC 4590 (M68)	-2.09	15.64	0.07

Notes to Table 2.

(1) All data from Armandroff (1989) except E(B-V) for NGC 362 which is from Peterson (1993), E(B-V) for M55 which is from Schade *et al.* (1988), and V(HB) and E(B-V) for M68 which are from Walker (1994). (2) V(RR) for 47 Tuc assumed to be 0.15 mag fainter than V(HB) in determining the apparent modulus.

tion can be carried out at two possible V magnitude intervals: either at magnitudes below the horizontal branch where contamination from stars evolving from the HB is not a concern, or at relatively bright magnitudes where, at least in galactic globular clusters, the AGB is no longer visible having either merged into the red giant branch or terminated. The fainter magnitude interval has the advantage of more stars but the photometric errors are larger, as is the degree of contamination from non-member objects (galactic foreground stars, M31 halo stars and background galaxies). The sensitivity to abundance is also reduced. Nevertheless, the mean B-V color for the 141 stars with $25.5 \leq V \leq 25.7$ and $0.66 \leq B-V \leq 1.02$ in Fig. 8 is 0.86 ± 0.01 , where the uncertainty given is the standard error of the mean. For the 166 stars with $25.7 \leq V \leq 25.9$ and the same color limits, the mean B-V color is also 0.86 ± 0.01 . The B-V color limits were chosen by inspecting histograms of the F450W-F555W color distributions for the equivalent F555W magnitude intervals in conjunction with the expected color error distributions. This allowed us to set limits which would comfortably include most possible members while excluding the majority of contaminating objects. Linear least squares fits to the B-V colors of the five standard globular cluster giant branches at $V = 25.6$ and $V = 25.8$ then enable the mean B-V

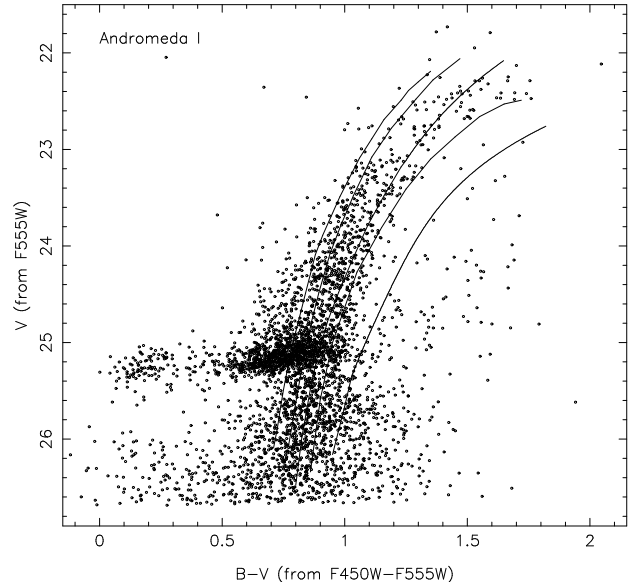


Fig. 8.— The (V, B-V) color-magnitude diagram for And I on which the giant branches for the standard galactic globular clusters M68 ([Fe/H] = -2.09), M55 (-1.82), NGC 6752 (-1.54), NGC 362 (-1.28) and 47 Tuc (-0.71) have been superposed. The adopted parameters for the galactic globular clusters are given in Table 2. The giant branches have been placed on the And I data assuming the $(M_V(HB), [Fe/H])$ relation of Lee *et al.* (1990) for $Y = 0.23$, an apparent distance modulus $(m - M)_V = 24.68$, and a reddening $E(B-V) = 0.04$ mag. The giant branches were then shifted a further 0.05 mag to the red (with no change in the V magnitudes) to improve the overall fit.

colors to be converted into abundance estimates. The resulting values are $[Fe/H] = -1.50 \pm 0.20$ and $[Fe/H] = -1.42 \pm 0.24$ for the brighter and fainter V magnitude intervals, respectively. The abundance uncertainties given include the error from the calibration, the statistical uncertainty in the observed mean color, and an adopted systematic uncertainty of ± 0.03 mag in the mean color. Together these values indicate an abundance for And I of $[Fe/H] = -1.45 \pm 0.20$ dex. This value is in good accord with that, $[Fe/H] = -1.4 \pm 0.2$, determined by MK90 from the mean (V-I)₀ color of And I's upper giant branch.

Inspection of the color-magnitude diagrams for the standard globular clusters indicates that AGB stars cease to be readily distinguishable from red giant branch stars brighter than $M_V \approx -1.5$, correspond-

ing to $V \approx 23.2$ in And I. We have therefore derived a second estimate for the mean abundance of And I by considering the mean (B–V) color of the stars in the magnitude intervals $22.5 \leq V \leq 22.7$, $22.7 \leq V \leq 22.9$, $22.9 \leq V \leq 23.1$, $23.1 \leq V \leq 23.3$ and $23.3 \leq V \leq 23.5$. Excluding a few obvious outliers, there are 23, 17, 13, 40 and 42 stars in these bins and, again using the standard globular cluster giant branches as calibration, the resulting mean abundances range from $[\text{Fe}/\text{H}] = -1.73$ to -1.64 dex, with uncertainties of order 0.25 dex. At these magnitudes, the abundance uncertainty is dominated by the uncertainty in the calibration rather than any systematic (assumed to be ± 0.03 mag) or statistical uncertainty in the mean B–V colors, though these have been included in the error calculation. Further, there is no systematic trend with luminosity in these upper giant branch abundance estimates, supporting our assertion that AGB stars have not biased the abundance estimates. We thus determine a mean abundance of $[\text{Fe}/\text{H}] = -1.67 \pm 0.25$ dex for And I from the upper giant branch stars.

This abundance is some 0.25 dex or so more metal-poor than that derived from the lower giant branch. It also differs by about the same amount from the abundance determination of MK90, which is based on the mean V–I colors of stars in a similar magnitude interval on the upper giant branch. Since we do not believe that AGB stars have significantly biased our result for the upper giant branch, the origin of this difference presumably lies with the F450W–F555W to B–V transformation. As noted above, the F450W–F555W to B–V transformation of H95b used here is derived synthetically from a spectrophotometric library of approximately solar abundance stars. It is therefore not surprising, given the difference in bandpass and effective wavelength between the F450W and B filters, that the differences in blanketing between solar abundance stars and metal-poor red giants can give rise to systematic errors. These effects are likely to be most marked for cooler redder stars and for that reason we prefer the And I abundance derived from the lower giant branch. Interestingly however, if we do not make the additional 0.05 mag shift in B–V color described above, then the abundance derived from the upper giant branch stars, $[\text{Fe}/\text{H}] = -1.55 \pm 0.25$ is in better accord with the value derived from the lower giant branch with the color shift applied (without the color shift, the lower giant branch yields an abundance of $[\text{Fe}/\text{H}] = -1.20 \pm 0.25$ dex). We therefore

adopt $[\text{Fe}/\text{H}] = -1.45 \pm 0.2$ dex as our best estimate of the mean abundance of And I, pending further investigation of the F450W–F555W to B–V transformation.

3.4. The Abundance Spread in And I

In section 3.1.3 we demonstrated that in the magnitude range $23.5 \geq F555W \geq 22.7$, the And I giant branch possesses an intrinsic color spread characterized by, for example, an (error corrected) standard deviation in the color residual from the mean giant branch of ~ 0.06 mag. We can now use the H95b transformations to B–V and the abundance calibrations derived above to convert these intrinsic F450W–F555W color residual measures to residual measures in abundance. We note in particular that since the abundance calibration is linear, the resulting abundance residuals do not depend on the mean abundance of And I, i.e. the validity of the 0.05 mag additional shift in B–V plays no role in the determination of the abundance residuals. Applying the transformations and the abundance calibrations then yields the following: $\sigma([\text{Fe}/\text{H}]) = 0.20$ dex, inter-quartile range 0.30 dex, central two-thirds of the sample abundance range 0.45 dex, and full abundance range for this sample of ~ 0.6 dex.

The abundance range for the central two-thirds of the abundance distribution determined here (0.45 dex) is considerably smaller than that (~ 1 dex) found by MK90. We attribute this difference principally to the fact that the superior resolution of HST and WFPC2 has produced colors and magnitudes with significantly smaller photometric errors over a similar magnitude interval to that used by MK90, resulting in less uncertainty in the derived abundance range. Specifically, MK90 determined the abundance range for the central two-thirds of their abundance distribution from an *observed* color range of ~ 0.4 in V–I with errors $\sigma_{V-I} \approx 0.13$ mag, dominated by image crowding. Our value comes from an observed F450W–F555W color range of 0.14 mag but with errors $\sigma_{F450W-F555W} = 0.02$ mag; the effect of the errors is thus considerably smaller in the present case.

Internal abundance spreads are well established in the galactic dSphs through both photometric and spectroscopic techniques. For example, Suntzeff (1993) lists values of $\sigma([\text{Fe}/\text{H}])$ for five systems ranging from ~ 0.2 to ~ 0.3 dex. Similarly, Armandroff *et al.* (1993) have photometrically determined $0.16 \leq \sigma([\text{Fe}/\text{H}]) \leq 0.24$ for the M31 dSph companion And III, while König *et al.* (1993) claim a large abundance disper-

sion, $\sigma([\text{Fe}/\text{H}]) \approx 0.43$, in the And II dSph galaxy. It is then apparent that the present result of $\sigma([\text{Fe}/\text{H}]) = 0.20$ dex for And I is one of the lower internal abundance dispersions measured in a dSph galaxy.

Naively one might expect that the abundance spread in a dSph galaxy would be larger in the higher mean abundance, higher luminosity (these two quantities are well correlated, e.g. Caldwell *et al.* 1992) systems, as more generations of stellar processing produce not only a higher mean abundance but also a higher abundance dispersion (see, for example, eq. 5 of Mould 1984). But this does not seem to be the case: among the And systems we see that And I and And III have similar values of $\sigma([\text{Fe}/\text{H}])$ while that of And II is apparently considerably larger, yet according to Caldwell *et al.* (1992), And I and And II have identical luminosities which exceed that of And III by approximately 1.5 magnitudes. Similarly, Suntzeff *et al.* (1993) have spectroscopically determined $\sigma([\text{Fe}/\text{H}]) = 0.19 \pm 0.02$ for the Sextans dSph, a value closely similar to that derived here for And I, yet Sextans is a dSph system that is ~ 1.7 magnitudes or more fainter than And I. Thus on the basis of presently available data, it is hard to make a compelling case that $\sigma([\text{Fe}/\text{H}])$ increases at all with luminosity among the M31 and galactic dSph companions. Clearly there is considerable scope for progress in this subject area, with large samples of spectroscopic abundance determinations, where practical, being the key ingredient. It may then be possible to use a ($\sigma([\text{Fe}/\text{H}])$, $[\text{Fe}/\text{H}]$ or M_V) correlation, or lack thereof, to constrain the formation and chemical evolution of these dwarf galaxies.

4. Discussion

4.1. And I and the Outer Halo of M31

The principal result of this study has been to reveal that the dSph galaxy And I, which lies in the outer halo of M31, has a predominantly red horizontal branch morphology. When combined with the metal abundance estimate $[\text{Fe}/\text{H}] = -1.45 \pm 0.2$ dex, this red HB morphology indicates that And I can be classified as a “second parameter” system; i.e. it possesses a redder HB than the majority of galactic globular clusters of comparable abundance. And I is thus similar to many of the galactic dSph galaxies which are also classified as second parameter objects.

In the Galaxy, second parameter systems (both globular clusters and dSphs) are most common in the

outer regions of the halo, while they are conspicuously absent from the inner halo region. *If* the second parameter effect is primarily driven by age differences, then this variation in the frequency of occurrence of the second parameter effect with galactocentric distance indicates that the mean age is smaller, and the age range larger, in the outer galactic halo (e.g. Lee *et al.* 1994; but see Richer *et al.* 1996 for an alternative view). This age variation interpretation is then one of the cornerstones of the halo formation model advocated initially by Searle & Zinn (1978; see also Zinn 1993b). In this model the outer halo is built up by mergers and accretions from a number of smaller independently evolving satellite galaxies.

While it is obviously premature to derive any strong conclusions from the observations of a single object, the existence of a second parameter system in the outer halo of M31, namely And I, is consistent with the hypothesis that the M31 outer halo formed by the same drawn-out chaotic process as postulated for the outer halo of the Galaxy. Certainly the lack of any substantial abundance gradient in the M31 globular cluster system (Huchra 1993) supports this contention¹⁰ though the most distant clusters studied are only at 25 - 30 kpc in projection from the center of M31 (*cf.* ~ 45 kpc for And I and up to ~ 100 kpc in the Galaxy). Similarly, the HB morphologies of the three metal-poor ($[\text{Fe}/\text{H}] \sim -1.8$ to -1.5 dex) M31 globular clusters studied by Fusi Pecci *et al.* (1996), which lie at projected distances of between ~ 15 and 20 kpc from the center of M31, do not show any obvious indication of second parameter characteristics. When combined with our result for And I, this is consistent with the diversity of HB morphologies expected as a consequence of the merger-accretion halo formation process. On the other hand, the mean abundance of the M31 halo population ($\langle [\text{Fe}/\text{H}] \rangle \approx -0.6$, Durrell *et al.* 1994) is considerably higher than that for the Galaxy. The M31 abundance would appear to be difficult to generate from the disruption of satellite galaxies unless the systems were predominantly more massive in the case of M31 than was the case for the Galaxy. It is worth noting though that dSphs with metal abundances comparable to the M31 halo mean abundance do exist. For example, the Sagittarius dSph galaxy, which is now merging into the halo of the Galaxy (Ibata *et al.* 1994), has a high mean abun-

¹⁰In the Galaxy, the lack of any radial abundance gradient in the halo globular cluster system is a second cornerstone of the postulated merger-accretion halo formation process.

dance; estimates range from $\langle[\text{Fe}/\text{H}]\rangle = -1.0 \pm 0.3$ (Ibata *et al.* 1994) to $\langle[\text{Fe}/\text{H}]\rangle = -0.5 \pm 0.1$ (Sarajedini & Layden 1995). Clearly then the comparatively high mean abundance for the halo field population in M31 is not a fatal objection to the merger-accretion halo formation process.

We are then in reality just beginning to explore the degree of similarity between the halo formation processes for the Galaxy and M31. Our present results for And I provide some support for the hypothesis that these halo formation processes were indeed similar, but many more objects in the outer halo of M31 with well determined HB morphologies and abundances are required before this issue can be settled.

4.2. The Age(s?) of And I

Turning now to And I itself, we first seek an estimate for the age of the majority population in this dSph. Over the past decade or more, studies reaching the main sequence turnoff in galactic dSphs have indicated that the age of the majority population varies substantially from dSph to dSph. Ursa Minor, for example, is apparently as old as the oldest galactic globular clusters (Olszewski & Aaronson 1985) while systems such as Carina (Mould & Aaronson 1983, Mighell 1990, Smecker-Hane *et al.* 1994) and Leo I (Lee *et al.* 1993b, Mateo *et al.* 1994) are dominated by stars of intermediate (~ 2 to 8 Gyr) age. For And I, observations reaching the main sequence turnoff ($V \approx 28.7$ for a population as old as most galactic globular clusters) are not currently practical and so we must seek alternate methods to provide an age estimate.

The most appropriate method is that of Sarajedini *et al.* (1995, hereafter SLL95; see also Hatzidimitriou 1991) which is based on the difference between the mean color of the giant branch at the level of the horizontal branch and that of the red HB. At fixed abundance, this color difference increases with increasing age. For And I, the lack of a clear separation between the red end of the HB and the giant branch (*cf.* Figs. 3 & 4) complicates the application of the SLL95 method. We have therefore proceeded as follows. First, to determine the mean color of the giant branch at the level of the horizontal branch ($V = 25.25$), we initially determined the mean giant branch color for the magnitude interval $25.4 \leq V \leq 25.8$, which lies just below the horizontal branch. We then employed the giant branches of the standard globular clusters NGC 362 and NGC 6752, which bracket And

I's mean abundance, to correct this mean color to a value appropriate for the magnitude of the horizontal branch. This process then yields $(B-V)_g = 0.88 \pm 0.02$ mag. Next, to determine the mean color of the red horizontal branch, we scaled the B-V color histogram for the giant branch in the magnitude interval $25.4 \leq V \leq 25.8$ by the relative number of stars on the red side of the equivalent histogram for the interval $25.0 \leq V \leq 25.4$, shifted it to the red by 0.03 mag to compensate for the giant branch slope, and then subtracted it from the distribution at the brighter magnitude interval. This generates a color distribution which is predominantly red HB stars. The mean color of this distribution is $\langle(B-V)_{HB}\rangle = 0.70 \pm 0.02$, where the error given incorporates both the uncertainty in the adopted scaling and in the color interval used to calculate the mean. These two mean values then give $d_{B-V} = 0.18 \pm 0.03$ mag.

Combining this determination with our adopted And I metal abundance of $[\text{Fe}/\text{H}] = -1.45 \pm 0.2$, Fig. 4 of SLL95 then yields an age for And I's majority population of 9.5 ± 2.5 Gyr. This age is younger than the ages of most of the galactic globular clusters, indeed it is even some 3 Gyr or so younger than the ages derived via this method for classic second parameter clusters such as NGC 362 (SLL95). It is not, however, inconsistent with the large spread of mean ages seen among the galactic dSphs. Nevertheless, it is reasonable to investigate the reliability of this age determination. We note first that the lack of any observed upper-AGB population in And I suggests strongly that there is no large population present with ages less than ~ 10 Gyr, which is consistent with the above result. Second, the recent HST based results of Mighell & Rich (1996) for Leo II provide an additional consistency check.

These authors present observations that reach fainter than the main sequence turnoff in this dSph, from which they conclude that the main stellar population in Leo II is 8 – 10 Gyr old. As noted above, this galactic dSph has a similar HB morphology to And I though its metal abundance is somewhat lower (Mighell & Rich (1996) give $[\text{Fe}/\text{H}] = -1.6 \pm 0.25$). Given this main sequence turnoff age determination, we can then apply the SLL95 method to the Leo II red HB and giant branch to see if consistent results are achieved. Mighell & Rich (1996) observed in the (F555W, F814W) system and they give $V-I = 0.828$ for the median color of the red HB and $V-I = 0.970$ for the color of the giant branch at the

level of the horizontal branch (note that these are observed, rather than reddening corrected values). The method of SLL95, however, requires B–V colors and so we have converted these V–I values to B–V using a linear relation between V–I and B–V that is based on the V–I photometry of Da Costa & Armandroff (1990) and the B–V photometry of Cannon & Stobie (1973) for giants in the globular cluster NGC 6752. This cluster has both similar reddening and similar abundance to Leo II. The transformation gives $(B-V)_g = 0.786$ and $\langle (B-V)_{HB} \rangle = 0.611$, yielding $d_{B-V} = 0.175^{11}$. Adopting $[\text{Fe}/\text{H}] = -1.6$ for the abundance of Leo II, this value of d_{B-V} yields an age of 8.5 Gyr from Fig. 4 of SLL95. This value is in excellent agreement with the results of Mighell & Rich (1996) who give, based on a number of methods principally based on the turnoff luminosity, a mean age of 9.1 ± 0.8 Gyr for Leo II’s dominant stellar population.

We conclude therefore that the SLL95 method as applied to our And I observations is relatively reliable and that therefore the bulk of the stellar population in this M31 dSph companion is approximately 10 Gyr old. In comparison with the galactic dSphs, this result indicates that And I is comparable to Leo II in age though it is definitely older than systems such as Carina and Leo I. It is probably somewhat younger than Sculptor, however, for which Da Costa (1984) has found an age some 2 to 3 Gyr younger than the majority of galactic globular clusters (in all these cases the age refers to the bulk of the stellar population).

One question remains. In Sections 3.1.3 and 3.4 we pointed out that And I has an intrinsic abundance dispersion. We have also shown that And I possesses a small (10 – 15%) population represented by blue HB and RR Lyrae variable stars. Is it possible that these blue HB stars and RR Lyrae variables result from the metal-poor tail of the abundance distribution at approximately constant age, or is it necessary to invoke a significant age difference between these stars and the bulk of the And I population? Again employing the HB models of Lee *et al.* (1994), it appears that at constant age, an abundance decrease of approximately 0.5 dex from $[\text{Fe}/\text{H}] \approx -1.5$ is needed to generate a reasonably blue HB (we assume $(B-R)/(B+V+R) = 0.5$). We therefore need to establish if the abundance

distribution in And I is compatible with a $\sim 10\%$ population that is approximately 0.5 dex more metal-poor than the mean. The results of Sect. 3.4 suggest that this is unlikely. The required abundance difference exceeds 2σ and for a gaussian distribution, only $\sim 2\%$ of the population is beyond that limit. Similarly, the size of the abundance range that contains 2/3rds of the sample, and the total observed abundance range, both suggest that a 10% sample containing the most metal-poor stars will differ from the mean abundance by only ~ 0.25 dex. This is not sufficient to generate a sufficiently blue horizontal branch. We conclude therefore that the blue HB and RR Lyrae stars are more readily explained as coming from a population that is somewhat older, by perhaps 3 Gyr or more, than the bulk of the And I population. This population may therefore be of comparable age to the globular clusters of the inner galactic halo.

There is, however, a possible caveat that should not go unmentioned. In Sect. 3.3 we noted that the mean abundance derived from the upper giant branch was approximately 0.2 to 0.25 dex more metal-poor than our preferred value. If this more metal-poor mean abundance was to be substantiated, then the low metal abundance tail of the abundance distribution could generate blue HB and RR Lyrae variable stars without requiring any substantial age difference. However, we do not believe this is the case. In addition to the arguments cited in Sect. 3.3 supporting the adoption of the higher abundance, we note that if the lower mean abundance for And I was correct, then the age derived from the d_{B-V} value would be ~ 8 Gyr. Such an age for the bulk of the stellar population in And I is inconsistent with the results that limit the intermediate-age (3 – 10 Gyr) population fraction in And I to $\sim 10 \pm 10\%$ (e.g. Armandroff *et al.* 1993, Armandroff 1994).

Consequently, we can restate our conclusion that the most reasonable explanation for the existence of blue HB and RR Lyrae variable stars in And I is that they represent a (small) population of stars that formed perhaps 3 Gyr or more before the bulk of the stellar population in And I. Such a result implies that, just as is the case for many of the galactic dSphs, star formation in And I occurred over an extended interval. The driving mechanism(s) behind the extended and diverse star formation histories of the Local Group dSph systems remains one of the most outstanding unsolved problems in this branch of Astronomy.

¹¹This value is slightly larger than that given by Mighell & Rich (1996), who used a quadratic (B–V, V–I) transformation derived from colors given in the Revised Yale Isochrones.

4.3. Horizontal Branch Morphology Radial Gradients

A further property of And I that is worthy of additional comment is that established in section 3.1.2: the existence of a radial gradient in the morphology of And I’s horizontal branch. The sense of the gradient is such that there are relatively more blue horizontal branch stars outside the core radius. This gradient could reflect either an underlying abundance gradient or a radial age gradient, but given the above discussion, it would seem more likely that it should be interpreted as suggesting that And I was more extended at its initial star forming epoch, than when the bulk of its stars formed.

In order to shed more light on this possibility, we have sought the existence of similar gradients in other dSph galaxies. This task requires dSph studies that fulfill the following criteria: a) the available photometry must extend beyond the core radius; b) the photometry must be reasonably precise at the magnitude of the horizontal branch; and c) the HB morphology must contain both blue and red stars. These criteria are satisfied by three studies: that of Carina by Smecker-Hane *et al.* (1994), of Leo II by Demers & Irwin (1993), and of Sculptor by Light (1988).

Considering first Carina, the extensive study of Smecker-Hane *et al.* (1994) clearly separates the “red clump” of intermediate-age core helium burning stars from the horizontal branch of old stars (both red and blue). Smecker-Hane *et al.* (1994) find no difference in the surface density distributions of these two classes of stars and further, they indicate that there is no systematic trend with radius in the fraction of the total core helium burning star population represented by the old HB stars. These results apply out to a radius of $\sim 10'$ beyond which their sampling is incomplete. Using the data of Irwin & Hatzidimitriou (1995, hereafter IH95), this limit corresponds to ~ 1.9 core radii on the major axis and ~ 2.8 core radii on the minor axis¹². Hence, while the use by Smecker-Hane *et al.* (1994) of circularly symmetric density profiles in this moderately flattened system ($\epsilon = 0.33$, IH95) may

have led to some loss of sensitivity to possible differences in the radial distributions of these two classes of stars, it is apparent that Carina differs from And I in lacking a HB morphology gradient.

For Leo II, we can analyze the data of Demers & Irwin (1993) in much the same way as was done for And I. This dSph is circularly symmetric (IH95) and, again using the results of IH95, the core radius is $1.7' \pm 0.4'$. From a number of different techniques, the center of this galaxy was found to be at (940, 1030) in the coordinate system of Demers & Irwin (1993). Then, defining red HB stars as those with $21.85 < V < 22.35$ and $0.45 \leq B-V \leq 0.65$, and blue HB stars as those with the same V magnitude range, but with $-0.2 \leq B-V \leq 0.4$ in the Demers & Irwin (1993) cmd study, we find $i = 0.20 \pm 0.02$ for the 275 HB stars ($b = 55$, $r = 220$) inside $1.7'$, and $i = 0.22 \pm 0.02$ for the 396 HB stars ($b = 87$, $r = 309$) outside this radius. The T_2 statistic (defined above) is 0.61 indicating no statistically significant difference in the horizontal branch morphologies. However, further investigation suggests that the HB morphology index for Leo II is approximately constant out to $r \approx 3.0'$, but beyond this radius the fraction of blue HB stars increases. For example, for $r \leq 3.0'$, $i = 0.20 \pm 0.02$ ($b = 112$, $r = 454$) while for $r \geq 3.0'$, $i = 0.29 \pm 0.04$ ($b = 30$, $r = 75$). Comparing these values yields $T_2 = 2.02$, or only a 2% probability of similar underlying HB morphologies. This result does not change significantly if the adopted center is changed by up to 20 pixels in either coordinate. Thus, while the statistical significance is not as high as it is for And I, there is a strong hint that the effect seen in And I is also present in Leo II. Unfortunately, the HST data of Mighell & Rich (1996) do not reach far enough from the center of Leo II to investigate whether or not the increased number of blue HB stars is accompanied by an increase of older stars in the vicinity of the main sequence turnoff.

Turning now to Sculptor, we note first that Da Costa (1984) pointed out that in his cmd, which was for a small area well outside the core, there were more blue HB stars than expected from scaling the cmd of Kunkel & Demers (1977), which applies to the central regions of this dSph. This result was followed up by Light (1988) who obtained intermediate band Gunn system CCD photometry at a number of locations in Sculptor. In his analysis, Light (1988) considered four circularly symmetric regions and calculated for each the ratio of the number of stars in two distinct

¹²We remind the reader that our use of the term “core radius” differs from that of IH95, for whom the term refers to the scale radius of the King (1966) model fit, rather than the radius at which the surface density reaches half its central value. The ratio of these two length scales is a function of the central concentration of the best-fit King model. In all cases, we have corrected the IH95 “core radius” to our convention by using the ratio appropriate for the central concentration listed by IH95.

areas in his cmd's. The first area contains the blue HB population ("blue" stars) while the second contains contributions from both the red HB and from the red giant branch ("red" stars). This situation was made necessary by the fact that the errors in his photometry did not permit a clean separation of the red HB from the red giant branch population at similar magnitudes. Further, again because of photometric precision concerns, the magnitude interval employed in defining these samples was overly generous, permitting additional numbers of red giant branch stars to contaminate the samples. The inclusion of such stars will dilute the effect of any radial gradient that is manifest only in the HB stars, as is the case in And I.

Based on the data of IH95, the core radius of Sculptor is $310'' \pm 80''$ on the major axis and $210'' \pm 60''$ on the minor axis. Consequently, Light's region 1 ($r \leq 210''$) is within the dSph's core radius for all position angles. Similarly, Light's regions 3 ($330'' \leq r \leq 480''$) and 4 ($r \geq 480''$) are completely outside the core. For region 1, there are 42 stars in the blue star area in the cmd and 234 in the red star area leading to a morphology index $i = 0.15 \pm 0.02$. For regions 3 and 4 together, blue HB stars are relatively more frequent with $i = 0.20 \pm 0.03$ ($b = 45$, $r = 182$). The T_2 statistic is 1.36 yielding a 9% probability that the samples are drawn from the same underlying distribution. If we consider only the outermost region, then again the blue HB stars are more frequent; $i = 0.28 \pm 0.07$ ($b = 10$, $r = 26$). Comparing with region 1, the T_2 statistic is 1.91 for a 3% probability that the samples are from similar distributions. Given the dilution effect of the inclusion of red giant branch stars in these samples, we regard these results as significant and conclude that, like And I and Leo II, Sculptor possesses a radial gradient in its HB morphology. Light (1988) reached the same conclusion. Clearly though, an extensive cmd study of Sculptor is required to place this conclusion on a firmer footing.

Thus in 2 of the 3 galactic dSphs considered, there are indications of similar HB morphology gradients to that seen in And I. Such a result should not be too surprising given the overall similarity between the M31 dSphs and the galactic dSph companions (e.g. Armandroff 1994). Nevertheless, the existence of a radial gradient in And I indicates that this dSph was more extended at its earliest star formation epoch. This in turn argues rather forcefully that And I formed and evolved as an independent system,

rather than as debris from the disruption of a larger system (as is sometimes argued for some, or indeed all, of the galactic dSphs, e.g. Lynden-Bell & Lynden-Bell 1995 and references therein).

5. Summary

In this paper we have presented results derived from WFPC2 images of the M31 dwarf spheroidal companion Andromeda I. The analysis has revealed for the first time the morphology of the horizontal branch in a dSph system beyond those that are satellites of our Galaxy. The And I HB morphology is predominantly red, which combined with our metal abundance estimate of $[\text{Fe}/\text{H}] = -1.45 \pm 0.2$ for this galaxy, indicates that And I can be classified as a second parameter object lying in the outer halo of M31. This result then offers support for the hypothesis that the halos of M31 and the Galaxy formed in a similar manner. The age of the majority population in And I is estimated as ~ 10 Gyr, though the occurrence of blue HB stars and RR Lyrae variables in the cmd is an indication of a minority population that is perhaps ~ 3 Gyr or more older. And I is therefore again similar to the galactic dSphs in having clear indications of an extended star formation history. The WFPC2 observations extend far enough from the center of And I to permit the discovery of a radial gradient in the HB morphology: the blue HB stars and RR Lyrae variables are relatively more common beyond And I's core. This result is interpreted as indicating that And I contracted between the epoch of the initial star formation episode and the time when the majority of the stars in the dSph formed. Similar HB morphology gradients were detected in two of three galactic dSphs studied. We have also derived the line-of-sight distance between And I and M31 as 0 ± 70 kpc and have verified the presence of an internal metal abundance spread within this dSph galaxy. The size of this metal abundance spread, however, is somewhat smaller than might have been expected on the basis of And I's luminosity. It will be interesting to see how these And I results compare with those for And II, a second M31 dSph companion which we will study with HST in Cycle 6.

G. Da C. would like to dedicate this paper to the memory of his father, who died while it was being written. His interest and support over the years will not be forgotten. G. Da C. is grateful for travel sup-

port from the Australian Government International Science & Technology Program “Space Science with the Hubble Space Telescope” and to Andrew Drake for discussions concerning the variable star periods. This research was also supported in part by NASA through grant number GO-05325 from the Space Telescope Science Institute, which is operated by AURA, Inc., under NASA contract NAS 5-26555.

REFERENCES

- Aaronson, M., Gordon, G., Mould, J., Olszewski, E., & Suntzeff, N. 1985, *ApJ*, 296, L7
- Ajhar, E.A., Grillmair, C.J., Lauer, T.R., Baum, W.A., Faber, S.M., Holtzman, J.A., Lynds, R., & O’Neil, E.J. 1996, *AJ*, 111, 1110
- Armandroff, T.E. 1989, *AJ*, 97, 375
- Armandroff, T.E. 1994, in *An ESO/OHP Workshop on Dwarf Galaxies*, edited by G. Meylan and P. Prugniel (ESO, Garching), p. 211
- Armandroff, T.E., Da Costa, G.S., Caldwell, N., & Seitzer, P. 1993, *AJ*, 106, 986
- Arnold, S.F. 1990, *Mathematical Statistics* (Prentice-Hall, Englewood Cliffs), p. 386
- Buonanno, R., Corsi, C.E., & Fusi Pecci, F. 1981, *MNRAS*, 196, 435
- Burstein, D., & Heiles, C. 1982, *AJ*, 87, 1165
- Caldwell, N., Armandroff, T.E., Seitzer, P., & Da Costa, G.S. 1992, *AJ*, 103, 840
- Cannon, R.D., & Stobie, R.S. 1973, *MNRAS*, 162, 227
- Casertano, S., Ratnatunga, K.U., Griffiths, R.E., Im, M., Neuschaefer, L.W., Ostrander, E.J., & Windhorst, R.A. 1995, *ApJ*, 453, 599
- Da Costa, G.S. 1984, *ApJ*, 285, 483
- Da Costa, G.S. 1992, in *The Stellar Populations of Galaxies*, IAU Symposium 149, edited by B. Barbuy and A. Renzini (Kluwer, Dordrecht), p. 191
- Da Costa, G.S., & Armandroff, T.E. 1990, *AJ*, 100, 162
- Demers, S., & Irwin, M.J. 1993, *MNRAS*, 261, 657
- Durrell, P.R., Harris, W.E., & Pritchet, C.J. 1994, *AJ*, 108, 2114
- Fusi Pecci, F., Ferraro, F.R., Corsi, C.E., Cacciari, C., & Buonanno, R. 1992, *AJ*, 104, 1831
- Fusi Pecci, F., Buonanno, R., Cacciari, C., Corsi, C.E., Djorgovski, S.G., Federici, L., Ferraro, F.R., Parmeggiani, G., & Rich, R.M. 1996, *AJ*, in press
- Gunn, J.E., & Stryker, L.L. 1983, *ApJS*, 52, 121
- Harris, W.E. 1982, *ApJS*, 50, 573
- Hatzidimitriou, D. 1991, *MNRAS*, 251, 545
- Hesser, J.E., Harris, W.E., VandenBerg, D.A., Allwright, J.W.B., Shott, P., & Stetson, P.B. 1987, *PASP*, 99, 739
- Holtzman, J., Hester, J.J., Casertano, S., Trauger, J.T., Watson, A.M., Ballester, G.E., Burrows, C.J., Clarke, J.T., Crisp, D., Evans, R.W., Gallagher, J.S., Griffiths, R.E., Hoessel, J.G., Matthews, L.D., Mould, J.R., Scowen, P.A., Stapelfeldt, K.R., & Westphal, J.A. 1995a, *PASP*, 107, 156 (H95a)
- Holtzman, J.A., Burrows, C.J., Casertano, S., Hester, J.J., Trauger, J.T., Watson, A.M., & Worthey, G. 1995b, *PASP*, 107, 1065 (H95b)
- Huchra, J.P. 1993, in *The Globular Cluster - Galaxy Connection*, ASP Conf. Ser. Vol. 48, edited by G.H. Smith and J.P. Brodie (ASP, San Francisco), p. 420
- Ibata, R.A., Gilmore, G., & Irwin, M.J. 1994, *Nature*, 370, 194
- Irwin, M., & Hatzidimitriou, D. 1995, *MNRAS*, 277, 1354 (IH95)
- Kaluzny, J., Kubiak, M., Szymański, M., Udalski, A., Krzemiński, W., & Mateo, M. 1995, *A&AS*, 112, 407
- King, I.R. 1962, *AJ*, 67, 471
- King, I.R. 1966, *AJ*, 71, 64
- König, C.H.B., Nemec, J.M., Mould, J.R., & Fahlman, G.G. 1993, *AJ*, 106, 1819
- Krist, J., & Hasan, H. 1993, in *Astronomical Data Analysis Software and Systems II*, ASP Conf. Ser. Vol. 52, edited by R.J. Hanisch, R.J.V. Brissenden and J. Barnes (ASP, San Francisco), p. 530
- Krist, J. 1994, *The Tiny Tim User’s Manual*, Version 4.0
- Kunkel, W.E., & Demers, S. 1977, *ApJ*, 214, 21
- Lee, M.G., Freedman, W.L., & Madore, B.F. 1993a, *ApJ*, 417, 553
- Lee, M.G., Freedman, W.L., Mateo, M., Thompson, I., Roth, M., & Ruiz, M.-T. 1993b, *AJ*, 106, 1420
- Lee, S.-W. 1977, *A&AS*, 29, 1

- Lee, Y.-W., Demarque, P., & Zinn, R. 1990, *ApJ*, 350, 155
- Lee, Y.-W., Demarque, P., & Zinn, R. 1994, *ApJ*, 423, 248
- Light, R.M. 1988, Ph.D. thesis, Yale University
- Lynden-Bell, D., & Lynden-Bell, R.M. 1995, *MNRAS*, 275, 429
- Mateo, M. 1996, in *Formation of the Galactic Halo....Inside and Out*, ASP Conf. Ser. Vol. 92, edited by H. Morrison and A. Sarajedini (ASP, San Francisco), p. 434
- Mateo, M., Olszewski, E.W., Pryor, C., Welch, D.L., & Fischer, P. 1993, *AJ*, 105, 510
- Mateo, M., Olszewski, E.W., Lee, M.-G., Saha, A., Hodge, P., Keane, M., Suntzeff, N., Freedman, W., & Thompson, I. 1994, *BAAS*, 26, 1395
- Mighell, K.J. 1990, *A&AS*, 82, 1
- Mighell, K.J., & Rich, R.M. 1996, *AJ*, 111, 777
- Mironov, A.V. 1973, *Soviet Ast.*, 17, 16
- Mould, J. 1984, *PASP*, 96, 773
- Mould, J., & Aaronson, M. 1983, *ApJ*, 273, 530
- Mould, J., & Kristian, J. 1986, *ApJ*, 305, 591
- Mould, J., & Kristian, J. 1990, *ApJ*, 354, 438 (MK90)
- Olszewski, E.W., & Aaronson, M. 1985, *AJ*, 90, 2221
- Peterson, C.J. 1993, in *Structure and Dynamics of Globular Clusters*, ASP Conf. Ser. Vol. 50, edited by S.G. Djorgovski and G. Meylan (ASP, San Francisco), p. 337
- Peterson, R.C., & Caldwell, N. 1993, *AJ*, 105, 1411
- Pritchett, C.J., & van den Bergh, S. 1988, *ApJ*, 331, 135
- Pritchett, C.J., & van den Bergh, S. 1994, *AJ*, 107, 1730
- Ratnatunga, K.U., & Bahcall, J.N. 1985, *ApJS*, 59, 63
- Richer, H.B., Harris, W.E., Fahlman, G.G., Bell, R.A., Bond, H.E., Hesser, J.E., Holland, S., Pryor, C., Stetson, P.B., Vandenberg, D.A., & van den Bergh, S. 1996, *ApJ*, 463, 602
- Ritchie, C. 1995, "Standard Star Monitoring", WFPC2 Calibration Monitoring Memo (Space Telescope Science Institute, Baltimore)
- Sarajedini, A., & Layden, A.C. 1995, *AJ*, 109, 1086
- Sarajedini, A., Lee, Y.-W., & Lee, D.-H. 1995, *ApJ*, 450, 712 (SLL95)
- Schade, D., Vandenberg, D.A., & Hartwick, F.D.A. 1988, *AJ*, 96, 1632
- Searle, L., & Zinn, R. 1978, *ApJ*, 225, 357
- Seitzer, P. 1985, in *Dynamics of Star Clusters*, IAU Symposium 113, edited by J. Goodman and P. Hut (Reidel, Dordrecht), p. 343
- Smecker-Hane, T.A., Stetson, P.B., Hesser, J.E., & Lehnert, M.D. 1994, *AJ*, 108, 507
- Suntzeff, N. 1993, in *The Globular Cluster - Galaxy Connection*, ASP Conf. Ser. Vol. 48, edited by G.H. Smith and J.P. Brodie (ASP, San Francisco), p. 167
- Suntzeff, N.B., Aaronson, M., Olszewski, E., & Cook, K.H. 1986, *AJ*, 91, 1091
- Suntzeff, N.B., Mateo, M., Terndrup, D.M., Olszewski, E.W., Geisler, D., & Weller, W. 1993, *ApJ*, 418, 208
- van den Bergh, S. 1995, *ApJ*, 446, 39
- Walker, A.R. 1994, *AJ*, 108, 555
- Zinn, R. 1993a, in *The Globular Cluster - Galaxy Connection*, ASP Conf. Ser. Vol. 48, edited by G.H. Smith and J.P. Brodie (ASP, San Francisco), p. 302
- Zinn, R. 1993b, in *The Globular Cluster - Galaxy Connection*, ASP Conf. Ser. Vol. 48, edited by G.H. Smith and J.P. Brodie (ASP, San Francisco), p. 38

This figure "Da_Costa.fig1.gif" is available in "gif" format from:

<http://arxiv.org/ps/astro-ph/9610083v1>